

**STEREOTYPE BASED STRESSORS IN GROUP CONTEXTS: THE ROLE OF
STRESS CONTAGION**

by

Rachel C. Amey

A thesis submitted to the Faculty of the University of Delaware in partial fulfillment of the requirements for the Master of Arts in Psychology

Fall 2019

© 2019 Rachel Amey
All Rights Reserved

**STEREOTYPE BASED STRESSORS IN GROUP CONTEXTS: THE ROLE OF
STRESS CONTAGION**

by

Rachel C. Amey

Approved: _____
Chad E. Forbes, Ph.D.
Professor in charge of thesis on behalf of the Advisory Committee

Approved: _____
Tania L. Roth, Ph.D.
Chair of the Department of Psychological and Brain Sciences

Approved: _____
John A. Pelesko, Ph.D.
Dean of the College of Arts and Sciences

Approved: _____
Douglas J. Doren, Ph.D.
Interim Vice Provost for Graduate and Professional Education and
Dean of the Graduate College

TABLE OF CONTENTS

LIST OF TABLES	v
LIST OF FIGURES	vi
ABSTRACT	vii

Chapter

1	INTRODUCTION	1
	Social Identity Threatening Contexts Induce Changes in Stress-Related Neural and Physiological Markers	1
	Stress Contagion in Group Contexts	5
	Performance Outcomes May Differ for those Directly Experiencing Stereotype Based Stress in Relation to Peers	7
2	STUDY OVERVIEW AND HYPOTHESES	9
	Hypothesis 1 (H1).....	9
	Hypothesis 2 (H2).....	10
	Hypothesis 3 (H3).....	10
	Hypothesis 4 (H4).....	11
3	METHODS.....	13
	Participants	13
	Procedure	14
	Interactive math task.....	15
	EEG recording.....	16
	EEG preprocessing.....	16
	Source reconstruction.....	17
	Functional connectivity estimation.....	18
	Select network modularity.....	19
	Functional connectivity estimation and network construction for MVPA analyses.....	20
	Processing performance feedback - MVPA classification.....	21
4	ANALYTIC STRATEGY	23

5	RESULTS.....	27
	Impact of SBS on Performance Over Time (H1)	27
	Impact of SBS on Neural Activity Over Time (H2).....	28
	Neural Indicators of SBS Contagion Over Time (H3)	30
	Effects of SBS Contagion on Performance (H4).....	33
	MVPA Classification Between DMT Actors and Partners	35
	MVPA Classification Between PST Actors and Partners	37
	MVPA Classification Between DMT Partners and PST Dyad Members ..	39
	Classification Between DMT Actors and PST Dyad Members	41
6	DISCUSSION.....	44
	REFERENCES	52
	Appendix	
A	SUPPLEMENTARY ANALYSES	67
B	INSTITUTIONAL REVIEW BOARD DOCUMENTATION	72

LIST OF TABLES

Table A.1	Hypothesis 1: SBSC Impacts Performance Interaction Breakdown	68
Table A.2	Hypothesis 1: SBSC Impacts Performance Simple Contrasts.....	68
Table A.3	Hypothesis 2: SBSC Promotes Changes in Neural Network Activity Interaction Breakdown	69
Table A.4	Hypothesis 2: SBSC Promotes Changes in Neural Network Activity Simple Contrasts.....	69
Table A.5	Hypothesis 3: SBSC Affects DMT Actors and Partners Interaction Breakdown.....	70
Table A.6	Hypothesis 3: SBSC Affects DMT Actors and Partners Simple Contrasts	71
Table A.7	Hypothesis 4: SBSC Predicts Underperformance Interaction Breakdown.....	71

LIST OF FIGURES

Figure 1	Neural hubs utilized in emotion saliency network connectivity analyses.....	4
Figure 2	Replication of participant set up.....	15
Figure 3	DMT partners perform worse overall; performance decreases over time while DMT actors are buffered, they do not underperform..	27
Figure 4	DMT actors threat response decreases over time to negative performance feedback; DMT partners exhibited greater vACC power to negative performance feedback across the entire task while DMT actor's activity decreased over time..	29
Figure 5	DMT partners demonstrate a stress contagion response; DMT actor's emotion saliency network connectivity on trial n predicts DMT partners emotion saliency network connectivity on trial n+1 to performance feedback.	32
Figure 6	DMT partners underperform as a result of SBS contagion; DMT partner's emotion saliency network connectivity on trial n predicts their underperformance on trial n+1 in the beginning of the task..	35
Figure 7	PLV t-test values between DMT actor and partner.	37
Figure 8	PLV t-test values between PST actor and partner.	39
Figure 9	PLV t-test values between DMT partners and PST dyad members.	41
Figure 10	PLV t-test values between DMT actors and PST dyad members.	43

ABSTRACT

Walk into any science, technology, engineering or mathematics (STEM) classroom and you're bound to find students solving problems together in groups. These group interactions may seem benign, if not successful forums for learning. However, these group-based contexts could be problematic for women since women are the targets of negative ability-oriented stereotypes in STEM domains. As such, these contexts may lead some women to experience stereotype based threats such as social identity threat; the fear that either themselves or others will be perceived in a way that confirms negative STEM stereotypes specific to their gender. Past research has extensively documented the negative downstream consequences of these threats on women in STEM, particularly with respect to the stress that these situations engender. This research, however, has occurred almost exclusively at the individual level, focusing on the people directly experiencing threat. Thus, a critical question is whether these stress-oriented consequences of stereotype-based threats experienced by individuals can undermine, or even be transmitted to otherwise non-threatened women during dyadic interactions. Utilizing neural and behavioral indices of dyadic synchrony, the current study examined whether social identity threatened women could transmit their stress to otherwise non-threatened women via a process we refer to as stereotype-based stress contagion (SBS Contagion), and how this collective stress affected women in a dyadic performance context. If threatened women can transmit their stress to otherwise non-threatened partners, does it hurt or benefit the

woman directly under threat, and, to what extent does this come at a cost to their otherwise non-threatened partners?

Chapter 1

INTRODUCTION

Social Identity Threatening Contexts Induce Changes in Stress-Related Neural and Physiological Markers

A large body of literature indicates that priming women in STEM settings with the stereotype that they are inferior to men in math causes various identity threats, including stereotype, collective, and social identity threat (SIT; Murphy, Steele, & Gross, 2007; Schmader, Johns, & Forbes, 2008; Cohen & Garcia, 2005). Importantly these identity threatening situations typically engender changes in stress-related biomarkers, including increased cortisol, blood pressure, and alpha amylase (Osborne, 2006; 2007; Blascovich, et al., 2001; Schmader, et al., 2009; Townsend et al., 2011). Identity threatening contexts are also clearly linked to neural correlates of negative stress-oriented emotional responses. For instance, women taking a supposed diagnostic math test in an identity threatening context exhibited increased ventral anterior cingulate (vACC) activation and non-linear amygdala responses, two regions prominently involved in the experience of stress, over the duration of a math task compared to men or women in identity safe contexts (Forbes et al., 2018; Liu et al., 2017; Krendl et al., 2008). We refer to these identity threat-based stress responses collectively as *stereotype-based stress (SBS)* responses.

More broadly, complex psychological phenomena, including SBS responses, are associated with characteristic whole brain patterns, and this whole brain pattern approach may help researchers further understand SBS responses. These relationships

have been observed using multi-voxel pattern analysis (MVPA, Nummenmaa & Saarimäki, 2017; Zhang et al., 2016; Liu et al., 2012) and neural network-based approaches. Complex psychological phenomena like SBS responses likely arise via interactions between regions across the whole brain and within specific functional networks (Bassett & Sporns, 2017; Mišić & Sporns, 2016). These interactions are defined by small or large scale alterations in communication within and between given brain networks underlying multiple psychological processes and behavioral outcomes (e.g., Harding, Yucel, Harrison, Pantelis, & Breakspear, 2015). For example, the experience of stress is associated with arousal-based activation of the amygdala, which initiates large scale interactions between brain regions comprising emotion and saliency networks (Bush et al., 2000; LaBar and Cabeza, 2006; Murty et al., 2010; Kim, 2011). Regions within the emotion-oriented network (that importantly are accessible via EEG) include dorsal and ventral aspects of the anterior cingulate (dACC; vACC), along with the prefrontal cortex (mPFC). Dorsal regions tend to be associated with appraisal and expression of negative emotions while ventral regions tend to be associated with regulation of these emotions (Etkin, Egner, & Kalisch; 2011). Regions within saliency and attentional control networks, such as the insula, inferior parietal lobe (IPL), and superior temporal sulcus (STS) (Dosenbach et al., 2007; Corbetta and Shulman, 2002; Seeley et al., 2007; Petersen and Sporns, 2015) are also commonly active in emotionally arousing contexts (Brooks et al., 2012; Viviani, 2013; Harenski & Hamann, 2006; Vuilleumier, 2005), especially those involving interactions with others (Figley, 2013; Nolte et al., 2013; Nummenmaa et al., 2008).

Previous work provides direct evidence for the benefits of utilizing a network approach to study stress in SBS contexts. Forbes et al. (2018) demonstrated that the

experience of stress in SBS contexts was associated with non-linear amygdala-based responses to emotionally evocative feedback. However, it was increased connectivity between two subnetworks of regions prominently involved in emotional memory encoding processes (one submodule consisted of the precuneus, dACC and bi-lateral insula sources while the second sub-module consisted of vACC, mPFC and bi-lateral MFG sources) that ultimately predicted the extent to which women accurately encoded the emotionally evocative feedback.

Given SBS contexts typically engender a variety of behavioral and physiological SBS responses (Blascovich et al., 2001; Osborne, 2006; Osborne, 2007; Schmader et al., 2009; Townsend et al., 2011), and that these responses are likely associated with unique network configurations, a network approach was utilized in the present study as a way to measure SBS responses. Enhanced connectivity between regions integral for emotion (dACC, vACC, and mPFC) in addition to regions implemented in saliency networks (IPL, insula, and STS) collectively could provide evidence for increased emotional processing and the detection and awareness of negatively arousing or stressful information. For brevity, we henceforth refer to these regions collectively as the ‘emotion saliency network’ (Figure 1), which builds on previous research highlighting the relationship between these two psychological constructs (emotion and saliency) in relation to the brain regions typically associated with these processes (Petersen & Sporns, 2015; Thompson & Fransson, 2017).

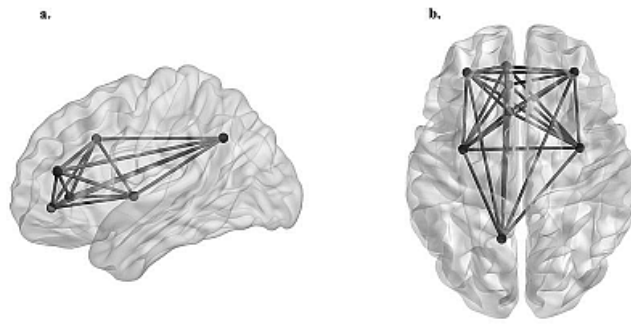


Figure 1 Neural hubs utilized in emotion saliency network connectivity analyses. a) Transverse view of emotion saliency network. b) Emotion saliency network viewed from the left hemisphere.

Stress Contagion in Group Contexts

While previous research provides evidence that social identity threatening contexts induce SBS responses for those directly experiencing the threat, it is entirely unclear what happens to other people who are in their presence. One possibility is that a woman directly experiencing SBS may transmit her SBS response to her otherwise non-stressed interaction partner. This transfer of negative stress-oriented emotions, may occur via a process referred to as emotion contagion, i.e., the phenomenon where one person's emotions and related behaviors directly trigger similar emotions and behaviors in other people to facilitate the transfer of moods among people in a group (Hatfield, Cacioppo, & Rapson, 1993; Barsade, 2002).

Stress-oriented emotions can be transmitted from one person to another via multiple channels, including voice, posture, facial expressions, and behaviors (Hatfield, Cacioppo, & Rapson, 1993; Decety et al., 2012). These contagion effects are even more robust in face-to-face interactions, where people readily assume the emotions of others. Importantly, this stress contagion can occur non-consciously and within minutes of partners interacting (West et al., 2017), engendering deleterious consequences for the dyad or group, such as hindered coordination and communication (e.g., withdrawal behavior; Waters et al., 2014). If social identity threatening contexts are indeed stressful, this suggests that the stress experienced by one partner can be transmitted to their partner via a contagion process, engendering stress in the other partner as well.

Like behavior and physiological synchrony studies, research on the neuroscience of social interactions reveals the brains of individuals within a dyad or group can synchronize with one another. For example, inter-brain synchronization has

been demonstrated between right centroparietal regions during social interactions in which participants mimic each other (Dumas et al., 2010), in the posterior superior temporal gyrus among speaker-listener pairs (Dikker et al., 2014), and in the right temporoparietal region within pairs of individuals who are cooperating or defecting in a social dilemma game (Jahng et al., 2017). Importantly, inter-brain synchronization has been associated with positive outcomes for performance and domain engagement. For instance, in classroom settings, better classroom engagement and social dynamics was found among students in a classroom to the extent they exhibited inter-brain synchrony with one another (Dikker et al., 2017; Bhattacharya, 2017). It's less clear *how* these positive brain synchrony-performance relationships manifest. Inter-brain synchronization in these studies was measured via spectral coherence across six channels that varied across subjects and were not differentiated in the analyses (i.e., which exact brain regions were synchronizing across individuals to affect performance was indeterminable). The present study expands on this work by utilizing an online network approach, operationalizing stress with vACC activity (power) and emotion saliency network connectivity. To the extent these neural regions are activated while individuals experience SBS and inter-brain synchronization occurs in social interactions, it's possible that individuals experiencing SBS may transmit their stress response to otherwise non-threatened individuals via synchronization between their respective emotion saliency networks. Such an approach provides a means to precisely monitor online neural synchrony on the order of milliseconds, while past contagion work has focused primarily on physiological and behavioral measures that collect samples on the order of seconds. This allows us to relate SBS contagion to behavioral outcomes like performance on a trial-by-trial basis.

Performance Outcomes May Differ for those Directly Experiencing Stereotype Based Stress in Relation to Peers

The social identity threat literature yields overwhelming evidence that social identity threat contexts have a detrimental effect on stigmatized individuals' performance and behaviors. However, it is much less clear how an otherwise non-threatened female interaction partner might change these outcomes or how these processes interact to affect the performance of both women in the dyad. Previous literature suggests both positive and negative potential effects on performance. For example, exposure to a female STEM role model buffers women's math performance in SBS contexts, and more role models result in even better performance (Lockwood & Kunda, 1997; Stout et al., 2011; Marx & Roman 2002; McIntyre et al., 2005). In addition, the gender composition of the group matters in group interactions and problem solving. Women in equal gender groups and female-majority groups do not exhibit SIT consistent outcomes. On the other hand, women in male majority groups reported feeling more anxious, participated less, and performed worse despite having the same task relevant knowledge (Dasgupta, Scircle, and Hunsinger 2015). Thus, from these perspectives, the presence of a non-SBS-threatened female interaction partner may buffer the effects of SIT on the woman directly experiencing SBS.

While there is some evidence that non-threatened female partners may have beneficial effects on performance and STEM perceptions of threatened individuals, past research suggests a more complex, nuanced, pattern may arise in dyadic interactions: women may have negative consequences on one another. When women were in the presence of women who embodied female STEM stereotypes or conformed to traditional female gender roles, they performed worse on a math task and their belief about their potential for success in STEM was diminished (Cheryan et

al., 2011; Deaux & Lewis, 1984; Fagot, 1977; Rudman & Fairchild, 2004). In addition, a recent study found the type of female partner present impacted performance among problem-solving dyads where either one or neither partner was directly experiencing SBS (Thorson et al., 2019). Specifically, math performance among partners of women directly experiencing SBS remained consistent over time. This was in contrast to women who were directly experiencing SBS whose performance improved over time. Thus, to the extent a woman may appear to initially embody traditional negative female STEM stereotypes during an interaction, or experience SBS, female peers interacting with these stereotype exemplars fail to improve their performance.

Chapter 2

STUDY OVERVIEW AND HYPOTHESES

The current study placed two female members of a single dyad in two adjacent EEG chambers. They communicated face-to-face via an iPad webcam. One member of the dyad, which we refer to as the *actor*, was told that they would be completing either a supposed diagnostic math test (DMT; an SBS context for women) or problem-solving task (PST; an SBS neutral context). The other member of the dyad, the *partner*, was *always* told that they would be completing a problem-solving task (thus yielding either DMT-PST dyads or PST-PST dyads, which we refer to as DMT or PST dyads for simplicity). Participants solved math problems together and received veridical positive and negative performance-related feedback after each problem while continuous EEG activity was recorded. We tested the following four hypotheses.

Hypothesis 1 (H1)

First, we wanted to demonstrate that SBS contagion occurs using a performance outcome. Competing hypotheses were proposed with respect to performance. On the one hand (H1a), SBS contagion could manifest such that both the actor and partner experience threat. In this case, DMT actors and their partners may have equally poor performance over time, and both DMT actors and their partners would underperform on the math task over time compared to PST dyad members. On the other hand, considering recent dyadic findings (Thorson et al., 2019) (H1b), SBS contagion could manifest such that the threat from the actor transfers completely to the partner. In this case, DMT actors may outperform their partners over time, and *only* their partners may underperform over time relative to PST dyad members. In addition,

DMT actors might improve their performance over time relative to PST dyads (Thorson et al., 2019).

Hypothesis 2 (H2)

Next, we wanted to demonstrate SBS contagion occurs with a neural measure as the outcome. Given the dyadic nature of this study (and the potential positive performance effects DMT partners may have on actors as described above), we hypothesized that neural-based SBS contagion effects would be evident in response to *both* positive and negative performance feedback. We expected DMT actors to exhibit increased vACC activity over time in response to all performance feedback received on the interactive math task in comparison to their partners and PST dyads. We also expected DMT partners to exhibit comparable levels of vACC activity over time relative to PST dyad members. Because past research finds consistent evidence that women experiencing SBS exhibit neural attentional and encoding biases only to stereotype confirming information like negative performance feedback, it is possible that the effects might be specific to negative feedback. We examine this possibility as well.

Hypothesis 3 (H3)

Next, we wanted to directly demonstrate that neural indicators of threat could be theoretically transferred from one person to the other by correlating the actor's neural responses to the partner's neural responses. We expected SBS to be transferred from the DMT actor to their partner over the course of the task; this was operationalized as increased emotion saliency network connectivity to performance feedback in actors predicting increases in the same measures of their partner on the

subsequent trial. We did not expect to find any neural based evidence of SBS transfer, also indexed by emotion saliency network connectivity correlations across partners, stemming from DMT partners to actors or in the PST dyads. Stereotype neutral contexts should be largely devoid of emotion or stress for women and should thus not engender SBS contagion. Like H2, we will first focus on all performance feedback types, but also explore the effects of negative feedback specifically.

Hypothesis 4 (H4)

Finally, we wanted to demonstrate that the neural transfer of SBS contagion has implications for performance. We expected that emotion saliency network connectivity would be directly tied to performance over time among partners in the DMT dyads. Specifically, heightened emotion saliency network connectivity in partners would predict underperformance on the following trial. We do not expect a relationship for DMT actors or PST dyad members.

In addition to looking at specific brain networks and regions as described above, neural based evidence for SBS contagion was further corroborated by examining the whole brain processing of performance feedback via MVPA. This data-driven approach statistically differentiates with varying levels of probabilistic confidence between brain patterns that are similar compared to those that are different. We expected that brain patterns and connectivity *within* DMT and PST dyads would be more similar, e.g., a given dyad would have more common hubs, or regions with high levels of connectivity, given that these actors and partners are working together to solve math problems. *Between* DMT and PST dyads, it's likely that fewer common hubs would be evident amongst these individuals given that they are wholly independent from one another, i.e., not working with one another. Therefore, if DMT

actors and their partners were truly exhibiting neural synchrony, their brain patterns should be indistinguishable from one another but distinguishable from dyads in the PST condition (particularly between *partners* in the DMT and PST conditions given the SBS-based differences between the actors they are paired with).

Chapter 3

METHODS

Participants

Fifty-eight white female students who granted written consent participated in the study for payment¹. Participants were recruited for the study if they expressed knowledge of the stereotype that men are better at math than women. Specifically, all participants responded with a three or lower to the following question during a pre-study screening: “Regardless of what you think, what is the stereotype that people have about women’s and men’s math ability” (1= Men are better than women; 7= Women are better than men). Participants were paired into twenty-nine dyads. One participant was excluded from EEG analyses due to a lack of valid trials, thus one (PST) dyad was removed from all dyadic analyses.

¹ Only white women who were biologically and self-identified as a woman were recruited for the study. This is because past research suggests that stigmatized ethnic minorities are susceptible to both math and intelligence based stereotypes in our society (Steele & Aronson, 1995; Beasley & Fischer, 2012; Gonzales, Blanton, & Williams, 2002). Given that stereotype threat can be primed in situations where minority individuals are outnumbered by ethnic majority members (aka “solo status” situations; Inzlicht & Ben-Zeev, 2000; Marx & Goff, 2005; Sekaquaptewa & Thompson, 2003) and the majority of the participant subject pool and most research assistants in our lab are white, there was a concern that race-related confounds would exist in multiple ways. We were also concerned about conditions that place men in situations where women normally experience stereotype threat. That is, if a stigmatized minority male is placed in the “stereotype threat” condition, they may also underperform, whereas white males typically do not underperform in these situations. Asian individuals also exhibit interesting and potentially confounding patterns, including performing better in stereotype threat situations (Shih, Pitinsky, & Ambady, 1999), if their ethnicity is primed (as would likely be the case if they find themselves in a solo status situation like they would in our study). Accordingly, for this initial foray into understanding SBS contagion, we focused on white female participants only. Expanding to other racial groups and genders is an important next step.

Procedure

Upon arrival to the lab, partners of each dyad met for the first time while signing consent forms; they were then prepared for EEG recording. Each member of the dyad was seated in their own soundproof chamber in front of a computer screen and iPad tablet. Dyads were randomly assigned to either a SBS/diagnostic math test condition (DMT, n=14 dyads) or a control/problem-solving task condition (PST, n=15 dyads). In the DMT condition, one participant (referred to as the “actor”) was exposed to SBS by being told they would complete tasks that were diagnostic of their math intelligence. They also completed demographic questions that included a gender query, had pre-recorded instructions read aloud to them in a male voice through headphones, and were prepped for EEG recording by at least one male experimenter. In contrast, the DMT actor’s interaction partner (referred to as the “partner”) and all participants in the PST condition were informed that they would be completing tasks that would inform researchers about the different types of problem-solving techniques they prefer (Forbes & Leitner, 2014; Forbes et al., 2015), completed demographic questions that excluded the gender query, had prerecorded instructions read aloud to them by a female voice through headphones, and were set up by female experimenters. Thus, DMT *partners* and both participants in the PST condition were always placed in stereotype neutral/stress-free contexts. That is, only the condition of the actor varied across dyad conditions. After an initial set of instructions, participants were connected via webcam on their iPad tablet in order to facilitate face-to-face communication during the interactive math task (described below). Participants were able to see one another through the duration of the interactive math task (Figure 2). When the interactive math task was completed, participants answered a series of questionnaires

alone (iPads were removed from the EEG chambers), were debriefed, and were compensated for their participation with cash or course credit.



Figure 2 Replication of participant set up. Participants were seated in an individual soundproof chamber. They were able to view their partner throughout the entire interactive math task through an iPad located below the synchronized computer screens.

Interactive math task. Actors and partners simultaneously completed a 100 problem math task consisting of standard multiplication and division problems (e.g., $10 \times 20 =$) that they solved both alone and together. Initial pilot tests confirmed that the problems selected varied in degree of difficulty (easy, medium and hard), ensuring all participants would solve problems correctly and incorrectly, thus exposing them to both positive and negative performance feedback. Actors and partners were first presented with the same math problem to solve alone for 16 seconds. During this solo time, participants were given three answer choices below each problem (A, B or C),

with the answer to each problem randomly presented in one of the three answer positions. Participants mentally completed all problems without scratch paper and made all answer selections via a button box placed in their laps. This solo answer was used for all performance outcomes in our analyses. After participants entered their solo answer, they were prompted with a screen that said, “Please discuss the answer to the problem with your partner”. At this time, participants were given 20 seconds to discuss their answer with their partner. Participants were then given five seconds to change or confirm their answer to the math problem they just solved alone. After submitting their final response, participants received feedback for two seconds that indicated whether their final answer was correct or incorrect (presented as the words “CORRECT” or “WRONG” written in black on a white screen).

EEG recording. Consistent with Forbes et al. (2018), continuous EEG activity was recorded from each member of the dyad using an ActiveTwo head cap and the ActiveTwo Biosemi system (BioSemi, Amsterdam, Netherlands). Recordings were collected from 64 Ag-AgCl scalp electrodes and from bilateral mastoids. Two electrodes were placed next to each other 1 cm below the right eye to record eye-blink responses. A ground electrode was established by BioSemi’s common Mode Sense active electrode and Driven Right Leg passive electrode. EEG activity was digitized with ActiView software (BioSemi) and sampled at 2048 Hz. Data was downsampled post-acquisition and analyzed at 512 Hz.

EEG preprocessing. For feedback analyses, the EEG signal was epoched and stimulus locked from 500ms pre-feedback presentation to 2000ms post-feedback presentation. EEG artifacts were removed via FASTER (Fully Automated Statistical Thresholding for EEG artifact Rejection; Nolan, et al., 2010), an automated approach

to cleaning EEG data that is based on multiple iterations of independent component and statistical thresholding analyses. Specifically, raw EEG data was initially filtered through a band-pass FIR filter between 0.3 and 55 Hz. Then EEG channels with significant unusual variance (absolute z score larger than 3 standard deviations from the average), mean correlations with other channels, and Hurst exponents were removed and interpolated from neighboring electrodes using a spherical spline interpolation function. EEG signals were then epoched and baseline corrected. Epochs with significant unusual amplitude range, variance, and channel deviation were removed. The remaining epochs were then transformed through ICA. Independent components with significant unusual correlations with EOG channels, spatial kurtosis, slope in the filter band, Hurst exponent, and median gradient were subtracted and the EEG signal was reconstructed using the remaining independent components. Finally, EEG channels within single epochs with significant unusual variance, median gradient, amplitude range, and channel deviation were removed and interpolated from neighboring electrodes within the same epochs.

Source reconstruction. All a priori sources used in network connectivity analyses were identified and calculated via forward and inverse models utilized by MNE-python (Gramfort et al., 2013 and Gramfort et al., 2014). The forward model solutions for all source locations located on the cortical sheet were computed using a 3-layered boundary element model (BEM; Hämäläinen and Sarvas, 1989), constrained by the default average template of anatomical MNI MRI. Cortical surfaces extracted with FreeSurfer were sub-sampled to approximately 10,240 equally spaced vertices on each hemisphere. The noise covariance matrix for each individual was estimated from the pre-stimulus EEG recordings after preprocessing. The forward solution, noise

covariance and source covariance matrices were used to calculate the dynamic statistical parametric mapping (dSPM) estimated inverse operator (Dale et al., 1999; Dale et al., 2000). The inverse computation was done using a loose orientation constraint (loose = 0.2, depth = 0.8) (Lin et al., 2006). Using depth weighting and noise normalization approaches, dSPM inverse operators have been reported to help characterize distortions in cortical and subcortical regions and improve the bias accuracy of neural generators in deeper structures, e.g., the insula (Attal & Schwartz, 2013). The cortical surface was divided into 68 anatomical regions (i.e., sources) of interest (ROIs; 34 in each hemisphere) based on the Desikan–Killiany atlas (Desikan et al., 2006) and signal within a seed voxel of each region was used to calculate the power within sources and phase locking (connectivity) between sources.

Functional connectivity estimation. Time series for all 68 sources were extracted using MNE for each presentation of performance feedback. Functional connectivity between two sources was computed via correlation; the band-power spectrum of all 68 sources within epochs was cross-correlated using Pearson's correlation coefficient (Chen, Ros, & Gruzelier, 2013). That is, for every trial of performance feedback, and within each frequency band, a symmetric 68×68 adjacency matrix was obtained. Consistent with previous studies focusing on over time physiological synchrony within dyads via heart rate and cortisol (Thorson & West, 2018; West et al., 2017; Dikker et al., 2017), a trial by trial approach was utilized in this study to capture the exact time course of SBS contagion. Trial by trial synchrony was assessed via actors and partners' connectivity within the *a priori* defined emotion saliency network (defined as select network modularity-see below; Forbes et al., 2018).

Given that phase-locking cannot be calculated for single trial data (multiple trials are needed for this calculation), functional brain networks were estimated from the signed correlation matrix, r_{ij} , as opposed to a phase locking matrix. Like the phase locking matrix however, this correlation matrix consists of both positive and negative edges, or functional connections. Positive edges between brain regions suggest synchrony over large-scale networks to facilitate dynamic links and integration functions. Negative edges have also been used in graph measures (Sporns and Betzel, 2016) and may reflect neurophysiologically relevant patterns (e.g., Rubinov and Sporns, 2011; Schwarz and McGonigle, 2011; Park & Friston 2013). However, they are also the subject of debate in terms of their origin, interpretation, relationship with structural connectivity, and possible neurophysiological function (Chen et al., 2011). For these reasons, negative edges were excluded from analyses and well-established algorithms that use only positive connections in the calculation of graph theoretical matrices were utilized (Rudie et al., 2013). This functional connectivity matrix was then converted to a sparse positive-only matrix by removing all negative weights. The remaining matrix was further pruned by applying a statistical threshold (Liu et al., 2011, 2013) to retain coefficients r_{ij} , that were less than or equal to half of the total positive connections.

Select network modularity. In the present study we utilized modularity analyses, or analyses that gauge the extent to which a set of nodes or brain regions in a functionally relevant network are interconnected and effectively communicate with one another compared to regions outside the network (Sporns, 2011). These analyses index how connectivity between regions in the emotion saliency network modulate task performance and neural connectivity in the partner's brain. Because of the trial-

by-trial nature of the over time analyses, select network modularity was modified from Forbes et al. (2018) such that between module connectivity was operationalized as correlations between pre-defined subnetworks, or other regions across the whole brain network, and within module connectivity was operationalized as the correlations between nodes within the emotion saliency network on a given trial. Because whole brain modularity values contain many subnetworks, while select network modularity focuses on a single subnetwork, and this measure compares this single subnetwork to many subnetworks (i.e., regions and connections) across the brain, select network modularity values become very small and often negative ($10E-4$). Thus, between and within module connectivity values were multiplied by 1000 to equate in magnitude select network values to conventional modularity values. Higher positive values indicate that the *a priori* defined network was more strongly connected compared to nodes outside the network of interest during a given trial. Lower negative values indicate that regions outside the *a priori* defined network may also be highly connected with one another (which is particularly likely when hubs are included in comparisons).

Figure 1

Functional connectivity estimation and network construction for MVPA analyses. Analyses conducted on the *a priori* emotion saliency network provide a sensitive assessment of how SBS contagion may unfurl on a trial-by-trial basis. However, it cannot be assumed that other neural regions or networks do not contribute to the SBS contagion process in a meaningful way. To address this, multivoxel pattern analyses (MVPA) were conducted on participants' data in a manner similar to past literature (Mahmoudi et al., 2012). Importantly, MVPA analyses examined neural activity to

performance feedback in the aggregate, i.e., on average as opposed to on a trial-by-trial basis. To obtain connectivity strength values for these analyses, phase locking values (PLV; Lachaux et al., 2000), which measure variability of phase between two signals across trials, were calculated (as opposed to the correlation matrix described above). PLV was measured by averaging the first 500ms after the onset of performance feedback collapsing across frequency bands (theta: 4-8hz, alpha: 9-14hz, beta:18-22hz, gamma:25-50hz). In other words, for every subject we obtained a symmetric 68×68 adjacency matrix of PLV between each source, representing the set of connections or edges in each participant's task-based connectivity profile.

Figure 2

Processing performance feedback - MVPA classification. Two training classes were implemented in the MVPA model consisting of participants in different conditions. For example, DMT actors would be one class while DMT partners would be the other class. Classifiers were constructed from these classes to distinguish between whole brain activity to performance feedback. This provided a means to observe the extent to which actors and partners processed performance feedback similarly or differently. Specifically, a whole brain connectivity network (based on PLV) was constructed for each participant during all performance feedback trials. During these analyses, a feature selection approach was taken. This approach determines which connections between varying brain regions are significant during performance feedback processing and can be used as features to represent connectivity differences between the two designated test groups (e.g., actors and partners). T-tests (e.g., Chen et al., 2016) were conducted on every connection between negative and positive classifiers across the whole brain. Connections corresponding to $p < 0.05$ were labeled as significant

connections. A support vector machine (SVM) classifier was then trained to maximally separate the two classifiers based on these data driven connections. After this separation, a classification accuracy score is given, i.e., a number is provided that describes how confidently these two groups can be classified from one another. To determine the reliability of the accuracy score, a significance test was conducted. Analyses were conducted to test the probability that this classification accuracy score was produced by chance (i.e., significantly different from 50%), or if it was the outcome of the given groups being truly distinct from one another.

Figure 3

Significance was determined via permutation testing; 1,000 permutations were run for each analysis. For all 1,000 permutations, the real classification rate from the original analysis was compared to the random classification rate. The random classification rate was constructed by shuffling participants into two equal groups and running an identical classification analysis. If the p-value was less than 0.05 when comparing classification accuracy from the actual groups to random assignment, results would suggest that the assigned groups from the study were able to be classified during feedback processing over and above random assignment.

Chapter 4

ANALYTIC STRATEGY

We tested hypotheses 1-4 using over time analyses that allowed us to examine changes that may occur due to SBS contagion over the course of the math task. To account for repeated measurements in individual and dyadic models, all analyses were conducted utilizing Generalized Estimating Equations (GEE; Ballinger, 2004; Liang & Zeger, 1986), specifying an exchangeable working correlation matrix (Fitzmaurice, Laird, & Rotnitzky, 1993, Fitzmaurice, Laird, & Ware, 2012, West, 2013). Across all hypotheses, condition was operationalized as DMT actor versus DMT partner versus PST dyad (a between-subjects factor), time was operationalized as trial number where trial 10 indicated the beginning portion of the task and trial 90 indicated the end portion of the task (a within-subjects factor), and feedback type was operationalized as positive versus negative (a within-subjects factor). Consistent with previous papers regarding frequency bands, all analyses concerning neural network predictors were conducted in the theta, beta, and gamma frequency bands; they are suggested to assess similar neural processes (i.e., excitatory neural activity; Axmacher, 2010; Dipoppa and Gutkin, 2013). Because three models were run for each analysis, multiple comparisons were accounted for using the Benjamini–Hochberg False Discovery Rate procedure (Benjamini, & Hochberg, 1995), using a q-level of .1 (Singh & Phillips 2010; Pintzinger et al., 2017). All presented results passed multiple comparison criteria.

H1: The first model sought to determine how SBS would impact performance over the course of the task in accordance with our competing hypotheses. In this analysis a logit model was specified given that the outcome variable for trial by trial performance is binary (correct coded 1; wrong coded 0). The full model included the

main effects of condition, time, and the two-way condition by time interaction as predictors of individuals' performance. We probed a significant condition by time interaction in two ways. First, we examined the simple slope of time for each condition. Second, we tested the simple contrast of condition for the beginning and end of the task.

H2: Operationalizing vACC power as a region-specific index of stress and with a goal of replicating past findings (Liu et al. 2017), the next model addressed the hypothesis that DMT actors and partners would exhibit evidence of SBS in the form of variation in vACC power to performance feedback. Specifically, this model included a condition by time by feedback type interaction, in addition to all lower order 2-way interactions and main effects predicting vACC power. A significant 3-way interaction was probed by examining the simple 2-way interaction for negative versus positive feedback. Significant simple 2-way interactions for feedback type were then probed in the following manner. We examined the simple slope of time for each condition and tested the simple contrast between conditions for the beginning and end of the task.

H3: The third model addressed the hypothesis neural indicators of threat could be transferred from one person to the other by correlating the actor's neural responses on trial n to the partner's responses on trial $n+1$ over time. To test this hypothesis, we constructed a GEE model with the 3-way interaction of condition, time, and a participant's own emotion saliency network connectivity on trial n , in addition to all lower order 2-way interactions and main effects predicting the other person's emotion saliency network connectivity on trial $n+1$. We also included the partner's emotion saliency network connectivity on trial n as a covariate to focus on the effect of the actor's emotion saliency network connectivity on the previous trial over and above the

partner's own connectivity. A significant 3-way interaction was probed by examining the simple 2-way time by network connectivity interaction for each condition. Significant simple 2-way interactions were probed in the following manner. We examined the simple slope of network connectivity for each condition at the beginning and end of the task. We also included negative and positive feedback models to explore whether effects were driven by negative or positive feedback specifically.

H4: The final model was designed to explore the hypothesis that SBS contagion affected the individual performance of actors and partners. SBS contagion was operationalized using the same variable as the third analysis: emotion saliency network connectivity to performance feedback. A logit model was specified given that the outcome variable for trial by trial performance is binary (correct coded 1; wrong coded 0). This model included the 3-way interaction of condition, time, and the individual's emotion saliency network connectivity on trial n , in addition to all lower order 2-way interactions and main effects as a predictor of their subsequent performance on trial $n + 1$. A significant 3-way interaction was probed by examining the simple 2-way network connectivity by time interaction for each condition. Significant simple 2-way interactions were probed by examining simple slopes of emotion saliency network connectivity at the beginning and end of the task.

MVPA: While we expected the emotion saliency network to play a large role in SBS contagion processes, the brain often utilizes multiple networks simultaneously. To observe whether there was additional evidence of SBS contagion not yoked to *a priori* defined emotion saliency networks or modularity measures, a data driven MVPA approach was employed to classify a given dyads' respective whole brain patterns in response to performance related feedback. MVPA analyses were conducted

on the following participant combinations: DMT actor vs. DMT partner, PST actor vs. PST partner, DMT partner vs. PST dyad member, DMT actor vs. PST dyad member. If two members of a dyad were processing feedback in a similar manner, the SVM classifier would not be able to distinguish between the two members; however, if two members of a dyad were processing feedback in different ways, a classifier would be able to successfully distinguish between the two. Thus, the following analyses were conducted in relation to the MVPA classifier generated for each dyad type: First, generally, we examined whether DMT actors and partners and PST actors and partners were *indistinguishable* from one another respectively. Then we examined whether DMT actors/partners compared to PST actors/partners should be *distinguishable* from one another. Moreover, neural regions that appear in these analyses may provide insight into whether SBS contagion was present in DMT dyadic interactions. If DMT dyad classification revealed a common hub associated with stress it would suggest that these dyads were experiencing a common stressor. Whole brain analyses on DMT dyads thus should also yield common hubs in the classifier traditionally implicated in emotional processing, e.g., vACC, whereas PST dyads should yield hubs in regions associated with executive function processing given the problem solving nature of the task.

Chapter 5

RESULTS

Impact of SBS on Performance Over Time (H1)

Initial examinations of performance revealed a condition by time interaction, $\text{Wald}\chi^2(2) = 13.72, p = .001$ (Figure 3). Specifically, DMT partner's performance decreased over time ($B = -.005$ ($SE = .002$); $\text{Wald}\chi^2(1) = 7.45$, (95% Wald LL CI = $-.009$; UL CI = $-.002$), $p = .006$; for every one unit increase in time (trial number), the log odds of getting the question correct decreased by .005 units.

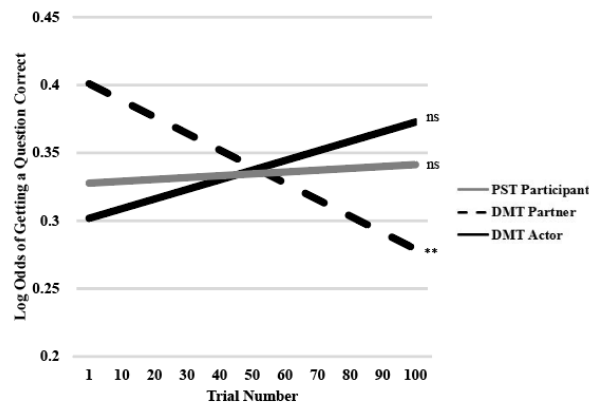


Figure 3 DMT partners perform worse overall; performance decreases over time while DMT actors are buffered, they do not underperform. This model tested H1 described in the text. It depicts the results of a model with the interaction between condition and time in addition to all main effects predicting performance. The significance tests in the figure correspond to the simple slope of time for each condition (*= $p < .05$, **= $p < .01$, ***= $p < .001$, ns=non-significant).

In contrast, DMT actors and PST dyad members exhibited no over-time changes, their performance remained stable (p 's > .11). Moreover, simple contrasts between conditions revealed performance differences between DMT actors and partners over the course of the task. At the beginning of the task, DMT partners had a higher probability of getting a question correct in comparison to the DMT actor ($p=.002$), and PST dyad members ($p=.034$). At the end of the task, DMT partners had a lower probability of getting a question correct in comparison to the partner ($p=.004$) and were largely comparable to PST dyad members ($p=.089$). DMT actors did not differ from PST dyad members ($p=.35$). Thus, at the end of the task, DMT partners underperformed in comparison to the actors. These findings support the possibility that DMT actors benefited from dyadic interactions at the expense of their partners.

Impact of SBS on Neural Activity Over Time (H2)

There was a marginally significant three-way interaction between condition, time, and feedback type predicting vACC activity to performance feedback in the gamma frequency band ($p=.09$; full statistics located in supplementary tables). As mentioned previously, we had a theoretical motivation to expect the effects might be specific to negative performance (Forbes & Leitner, 2014; Forbes et al., 2015; Forbes et al., 2018; Mangels et al. 2011). Accordingly, we probed the marginal 3-way interaction to test whether there were differences according to type of feedback (negative versus positive).

The 3-way interaction was driven by vACC power in response to negative performance feedback. Specifically, there was no 2-way condition by time interaction for positive feedback, $p=.83$. However, there was a significant condition by time interaction for negative feedback (Wald $\chi^2(2) = 9.75$, $p = .00004$, Figure 4). Observing

the simple 2-way condition by time interaction for negative performance feedback revealed that vACC activity did not change over time for DMT partners or PST dyad members ($p > .18$). Testing the simple slope of time for DMT actors revealed that DMT actor's vACC activity, decreased over time ($B = -.005$, $SE = .001$, $Wald\chi^2(1) = 16.69$, $p < .01$ (95% Wald LL CI = $-.007$; UL CI = $-.002$)).

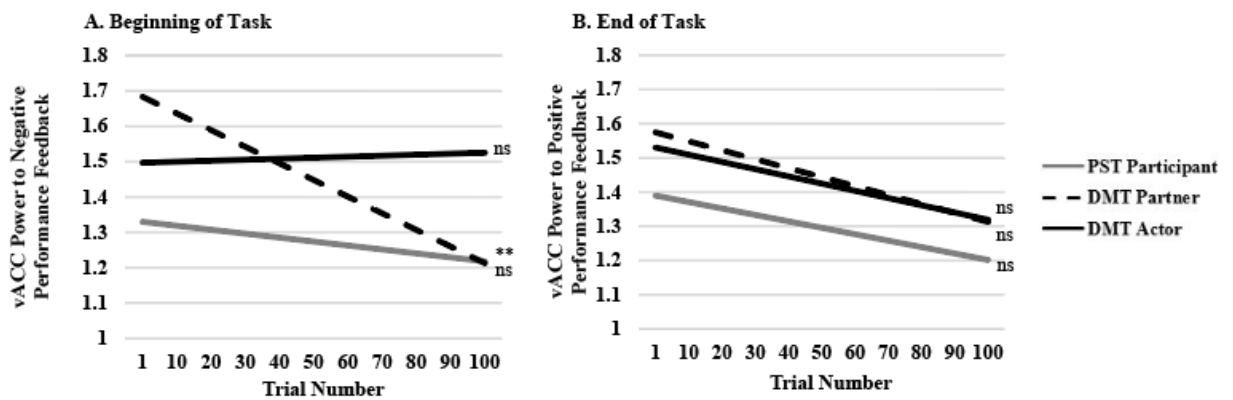


Figure 4 DMT actors threat response decreases over time to negative performance feedback; DMT partners exhibited greater vACC power to negative performance feedback across the entire task while DMT actor's activity decreased over time. This model tested H2 described in the text. It depicts the results of a model with the interaction between condition, time, and feedback type, in addition to all lower order 2-way interactions and main effects predicting vACC power over time. Panel A depicts the simple 2-way interaction between condition and time for negative performance feedback. Panel B depicts the simple 2-way interaction between condition and time for positive performance feedback. The significance tests in the figure correspond to the simple slope of time for each condition (*= $p < .05$, **= $p < .01$, ***= $p < .001$, ns=non-significant).

Simple contrasts across conditions revealed that, in the beginning of the task, DMT actors had comparable vACC power to negative performance feedback relative to DMT partners ($p=.12$). However, both DMT actors and partners exhibited higher vACC power to negative performance feedback in comparison to PST dyad members ($p's<.01$). By the end of the task, DMT partner's vACC power was greater than that of DMT actor's ($p=.001$). DMT partner's vACC power was also greater than PST dyad participants ($p<.000004$), while DMT actor's vACC power was comparable to PST dyad members ($p=.63$). Comparisons in vACC power to negative performance feedback thus suggests that DMT actors experienced an initial neural stress response that steadily decreased over time, whereas DMT partners experienced a steady stress response throughout the task, greater than that exhibited by PST dyad members, despite not initially being placed in a SBS context themselves.

Neural Indicators of SBS Contagion Over Time (H3)

The 3-way interaction between condition, time, and the participant's own emotion saliency network connectivity to performance feedback on trial n predicting the other person's emotion saliency network connectivity on trial $n + 1$ was significant in the theta frequency band (Wald $\chi^2(2) = 7.13, p = .028$, Figure 5). We first focused on the simple 2-way interaction of time and network connectivity for each condition. The 2-way time by network connectivity interaction was non-significant for both the DMT partners and PST dyads predicting their interaction partner's network connectivity ($p's>.12$). However, the 2-way time by network connectivity interaction was significant for the DMT actors predicting their partner's network connectivity ($b=.002, SE=.0001, \text{Wald } \chi^2(1) = 3.88, 95\% \text{ CI } [.00001, .004], p=.049$). Simple slopes of network connectivity demonstrated that in the beginning of the task, lower DMT

actor's network connectivity on trial n marginally predicted higher partner's network connectivity on trial n+1 ($b=-.087$, $SE=.047$, Wald $\chi^2(1) = 3.47$, 95%CI $[-.179, .005]$, $p=.06$). In contrast, by the end of the task, DMT actor's and their partner's network connectivity were unrelated ($p=.18$). These results provide evidence for SBS contagion in contexts where one individual initially experiences SBS and suggests that contagion begins very quickly after the task begins.

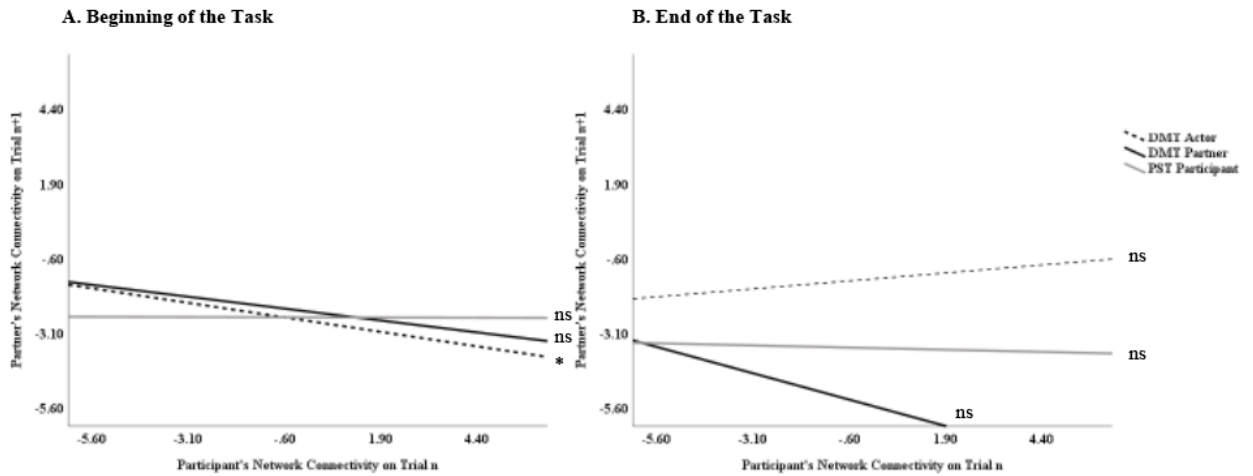


Figure 5 DMT partners demonstrate a stress contagion response; DMT actor's emotion saliency network connectivity on trial n predicts DMT partners emotion saliency network connectivity on trial n+1 to performance feedback. This model describes H3 in the text. It depicts the results of a model with the interaction between condition, time, and the participant's own emotion saliency network connectivity on trial n, in addition to all lower order 2-way interactions and main effects predicting other person's emotion saliency network connectivity on trial n+1. This model also included the partner's emotion saliency network connectivity on trial n as a covariate to focus on the effect of the actor's emotion saliency network connectivity on the previous trial over and above the partner's own connectivity. Panel A depicts the simple 2-way interaction between condition and a participant's own emotion saliency network connectivity during trial n on their partners network connectivity on trial n+1 for the beginning of the task. Panel B depicts the same simple 2-way interaction for the end of the task. The significance tests in the figure correspond to the simple slope of time for each condition (*= $p < .05$, **= $p < .01$, ***= $p < .001$, ns=non-significant).

Although DMT actor's network connectivity on trial n predicted DMT partner's network connectivity on trial n+1 for all performance feedback across the task, consistent with vACC patterns, these patterns were largely driven by brain

activity elicited in response to negative performance feedback. Despite a non-significant three way interaction ($p=.11$), we decided to look for continuous evidence of this trend with negative feedback. Like H2, there were no effects for positive performance (p 's $< .10$). However, there was a two-way interaction between DMT actors' emotion saliency network connectivity on trial n and time, predicting DMT partners network connectivity on trial $n + 1$ ($b=.003$, $SE=.0017$, Wald $\chi^2(1) = 4.11$, 95% CI [.0001, .007], $p=.06$) for negative feedback only. Relationships between PST dyad members, and for DMT partners, predicting DMT actors were not significant (p 's $> .46$).

Effects of SBS Contagion on Performance (H4)

There was a marginally significant three-way interaction between condition, time, and emotion saliency network connectivity on trial n predicting performance on trial $n + 1$ ($p=.09$). Once again, however, these effects appeared to be driven by emotion saliency network connectivity in response to negative performance feedback, just as they were with H2 and H3. This was unsurprising considering we had a theoretical motivation to expect the effects might be specific to negative performance (Forbes & Leitner, 2014; Forbes et al., 2015; Forbes et al., 2018; Mangels et al., 2011). Using the same rationale as H3, a model including only negative performance feedback revealed a significant 3-way interaction of condition, time, and the participant's own emotion saliency network connectivity on trial n predicting their performance on trial $n + 1$ in the theta frequency band (Wald $\chi^2(2) = 7.89$, $p = .019$, Figure 6).

We first probed the simple 2-way interaction of time and network connectivity for each condition. The 2-way time by network connectivity interaction was not

significant for both the DMT actors and PST dyad members predicting their performance on the following math trial ($p's > .09$). However, the 2-way time by network connectivity interaction was significant for the DMT partners predicting their own performance on the following trial ($b = .001$, $SE = .0006$, Wald $\chi^2(1) = 4.79$, 95% CI $[-.0001, .002]$, $p = .028$).

We also focused on the 2-way condition by network connectivity interaction for the beginning versus the end of the task. Simple slopes of network connectivity demonstrated that in the beginning of the task, higher DMT partner's connectivity on trial n predicted their underperformance on trial $n + 1$ ($b = -.071$, $SE = .027$, Wald $\chi^2(1) = 6.556$, 95% CI $[-.125, -.017]$, $p = .01$). In contrast, by the end of the task, DMT partners network connectivity had no effect on their performance ($p = .26$). This suggests that the product of SBS contagion, operationalized as emotion saliency network connectivity to feedback in comparison to whole brain activity, may specifically affect the performance of those interacting with individuals initially experiencing a SBS response.

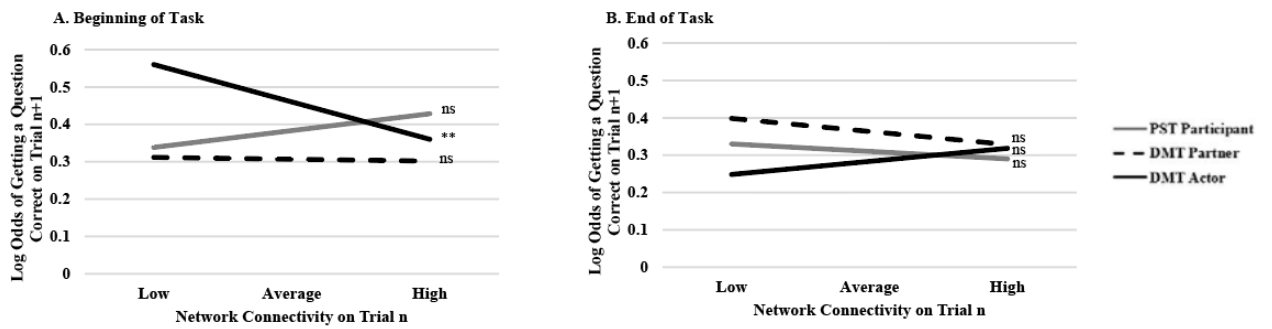


Figure 6 DMT partners underperform as a result of SBS contagion; DMT partner’s emotion saliency network connectivity on trial n predicts their underperformance on trial n+1 in the beginning of the task. This model describes H4 in the text. It depicts the results of a model with the interaction between condition, time, and the individual’s emotion saliency network connectivity on trial n, in addition to all lower order 2-way interactions and main effects predicting their subsequent performance on trial n + 1. Panel A depicts the simple 2-way interaction between condition and the participant’s own emotion saliency network connectivity on trial n for the beginning of the task. Panel B depicts this simple 2-way interaction for the end of the task. In both panels low and high connectivity correspond to +/- 1 standard deviation of network connectivity. The significance tests in the figure correspond to the simple slope of time for each condition (*=p<.05, **=p<.01, ***=p<.001, ns=non-significant).

MVPA Classification Between DMT Actors and Partners

Previous analyses specific to SBS contagion were constrained to an *a priori* defined emotion saliency network and vACC but it’s possible that SBS contagion effects transcend these a priori defined parameters. Thus data-driven based MVPA analyses were conducted to probe for whole brain patterns that may corroborate network based analyses. SVM models were first run to observe if there were any differences in feedback processing between actors and partners within DMT dyads. Within these dyads, 194 statistically significant whole brain connections were found

(connections presented in Figure 7). Regions with the most meaningful connectivity, or hubs defined by five or more significant connections in the corresponding hemispheres (L/R; Left, Right), were as follows: Parahippocampal Gyrus (L), Parstriangularis (L), Posterior Cingulate Cortex (R), vACC (or R Rostral Anterior Cingulate), Rostral Middle Frontal Cortex(L/R), Superior Frontal Gyrus (R), Supramarginal Gyrus (L/R), Temporal Pole(L/R), Transverse Temporal Cortex (L/R) (Figure 7). Not surprisingly, given that actors and partners were jointly working together on difficult math problems, most of these hubs are implicated as integral for executive function and attentional processes (i.e., Superior Frontal Gyrus, Parahippocampal gyrus, Parstriangularis, Rostral Middle Frontal Cortex, Temporal Pole, Transverse Temporal Cortex; Alvarez & Emory,2006; Raye et al., 2007; Hopfinger, Buonocore, & Mangun, 2000; Cohen et al., 1997; Hampshire et al., 2010). Importantly vACC (Rostral Anterior Cingulate) was also identified in this analysis, which, consistent with a priori analyses, suggests a similar stress response was evident among members of DMT dyads.

While identified hubs were consistent with executive function and emotional processes, the classification rate from the SVM model was .40, meaning only 40% of participants within these groups could be classified to their respective conditions (DMT actor or partner). After permutation testing, classification was confirmed to be unreliable in classifying between DMT actors and partners ($p > .05$). Overall this suggests that members of DMT dyads were processing performance feedback in a similar manner, despite being in different conditions from the outset.

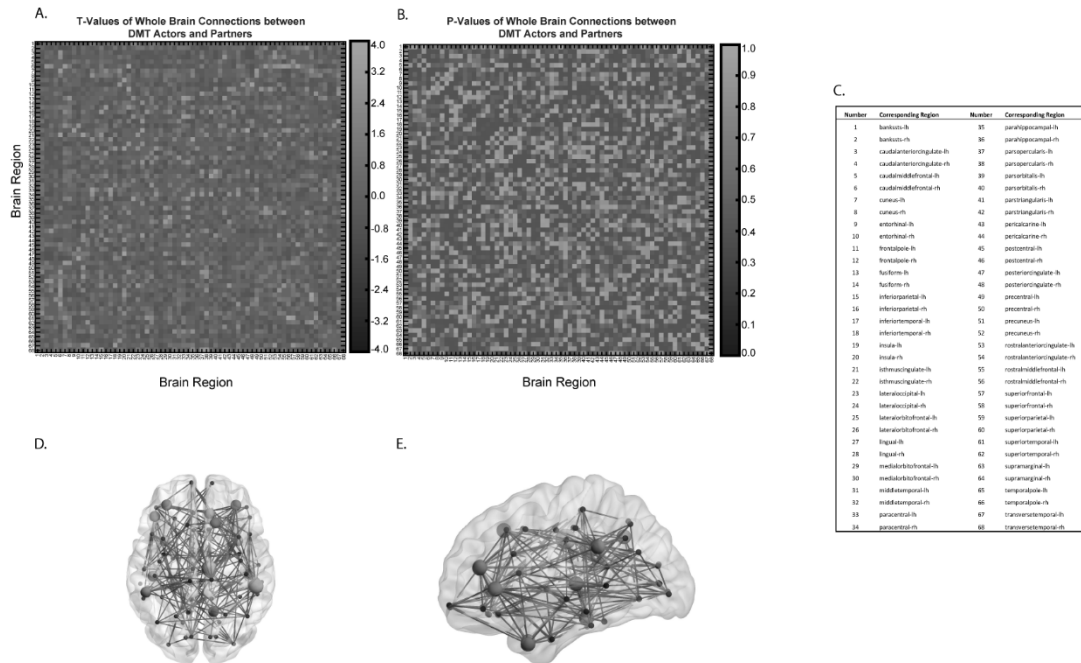


Figure 7 A) PLV t-test values between DMT actor and partner. Black shades indicate negative correlations, grey shades indicate positive correlations. B) PLV significant values between DMT actor and partner. Black shades indicate $p < .05$. C) Corresponding neural regions for matrices A and B. D) Neural distribution of significant hubs and connections between DMT actors and partners; horizontal plane. Larger hubs indicate increased connectivity with other regions. E) Neural distribution of significant hubs and connections between DMT actors and partners; sagittal plane. Larger hubs indicate increased connectivity with other regions.

MVPA Classification Between PST Actors and Partners

Identical analyses were run on SVM models for PST dyad participants. Within PST dyads, 200 statistically significant whole brain connections were found (connections presented in Figure 8). Regions with the most meaningful connectivity, or hubs defined by five or more significant connections, were as follows: Insula (R), Parahippocampal Gyrus (L), Parstriangularis (R), Pericalcarine Sulcus (L/R), Post Central Gyrus (L/R), Posterior Cingulate Cortex (L), Precentral Gyrus (L/R), Rostral

Middle Frontal Cortex (R), Superior Parietal Cortex (R), Supramarginal Gyrus (R), Temporal Pole (R), Transverse Temporal Cortex (L/R) (Figure 8). Similar to DMT dyads, the model revealed that PST dyads demonstrated numerous hubs that are often implicated in supporting executive function and attentional processes (i.e., Parahippocampal gyrus, Parstriangularis, Rostral Middle Frontal Cortex, Insula, Temporal Pole, Transverse Temporal Cortex; Alvarez & Emory, 2006; Raye et al., 2007; Hopfinger, Buonocore, & Mangun, 2000; Cohen et al., 1997; Hampshire et al., 2010). It is also important to note that given that both dyads were completing an identical task, similar regions were identified in PST and DMT dyads. One of the chief differences was that vACC was identified in DMT dyads, whereas it was *not* identified in PST dyads. This is what would be expected if one group was solving problems in a more stressful context.

The classification rate from the SVM model was .61, meaning 61% of participants within these groups could be classified to their respective conditions. After permutation testing, classification was confirmed to be unreliable in classifying between PST actors and partners ($p > .05$). Overall this suggests that members of PST dyads were processing performance feedback in a similar manner as participants were unable to be classified from one another at a rate that was more meaningful than if participants were randomly assigned.

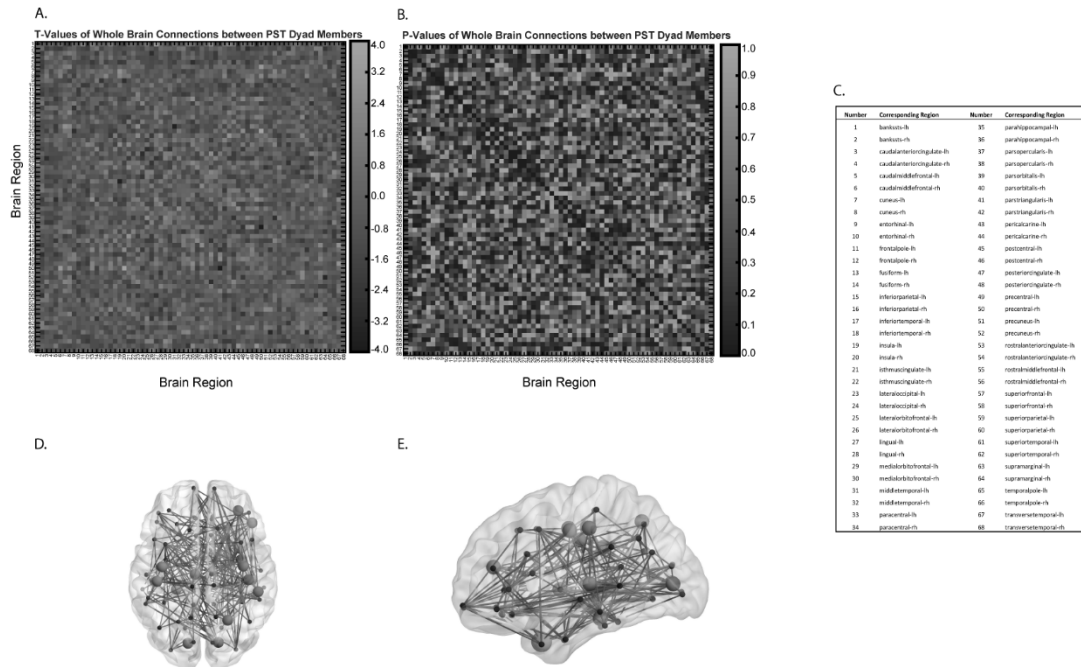


Figure 8 A) PLV t-test values between PST actor and partner. Black shades indicate negative correlations, grey shades indicate positive correlations. B) PLV significant values between PST actor and partner. Black shades indicate $p < .05$. C) Corresponding neural regions for matrices A and B. D) Neural distribution of significant hubs and connections between PST actors and partners; horizontal plane. Larger hubs indicate increased connectivity with other regions. E) Neural distribution of significant hubs and connections between PST actors and partners; sagittal plane. Larger hubs indicate increased connectivity with other regions.

MVPA Classification Between DMT Partners and PST Dyad Members

SVM models were then run to determine if there were any differences in feedback processing between DMT partners and PST partners. The only difference between these two groups was who they were paired with throughout the task. Successful classification between the two would suggest being paired with a female

actor experiencing threat may affect the partner differently than if they were paired with a non-threatened partner. Within DMT dyads, 123 statistically significant whole brain connections were found (connections presented in Figure 9). Regions with the most meaningful connectivity, or hubs defined by five or more significant connections, were as follows: Pericalcarine Sulcus (L), Precentral Gyrus (R), Rostral Middle Frontal Gyrus (L), Superior Temporal Gyrus (L), and Supramarginal Gyrus (L/R) (Figure 9). Fewer meaningful hubs were identified between members of DMT and PST dyads, which was expected given these two groups, while working on an identical task, ultimately belonged to different dyads.

Importantly, the classification rate from the SVM model was .81, meaning 81% of participants within these groups could be classified to their respective conditions. After permutation testing this rate was deemed significant ($p < .05$); partners of PST and DMT dyads were able to be successfully classified from one another, suggesting members of these different dyads were processing performance feedback in a different manner. This provides additional data driven, whole brain, evidence for the presence of SBS contagion in DMT dyads given that the only difference between these individuals was the condition of the actor they were working with (i.e., they received identical instructions at the beginning of the task whereas their partners did not).

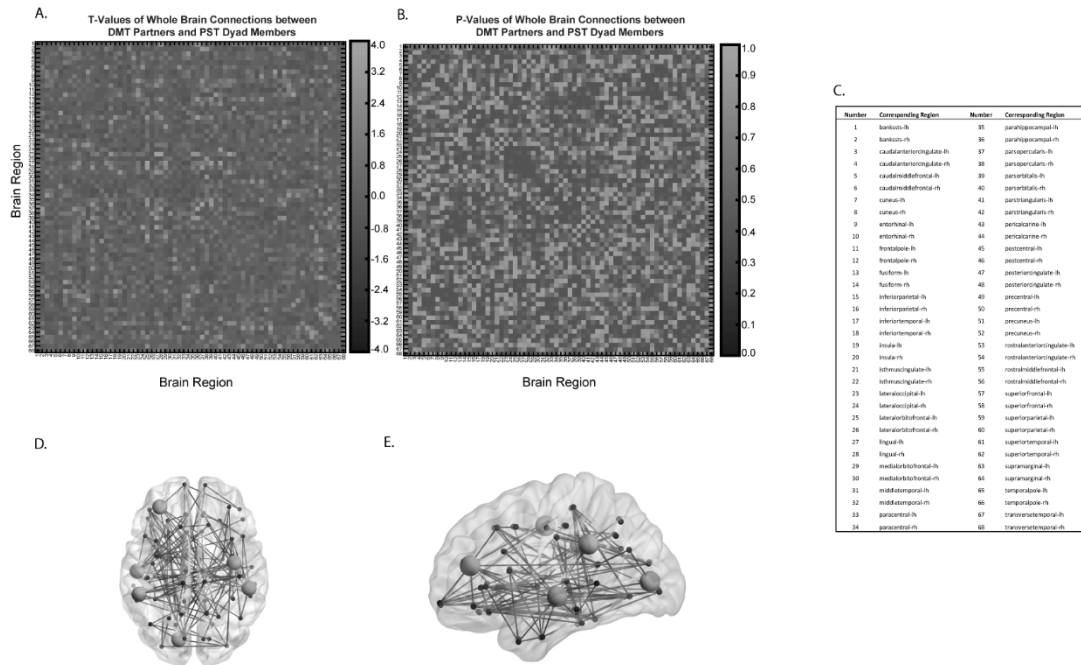


Figure 9 A) PLV t-test values between DMT partners and PST dyad members. Black shades indicate negative correlations, gray shades indicate positive correlations. B) PLV significant values between DMT partners and PST dyad members. Black shades indicate $p < .05$. C) Corresponding neural regions for matrices A and B. D) Neural distribution of significant hubs and connections between DMT partners and PST dyad members; horizontal plane. Larger hubs indicate increased connectivity with other regions. E) Neural distribution of significant hubs and connections between DMT actors and partners; sagittal plane. Larger hubs indicate increased connectivity with other regions.

Classification Between DMT Actors and PST Dyad Members

Follow up SVM models were run to determine if there were any differences in feedback processing between DMT actors and PST partners. If DMT partners truly buffered DMT actors, as performance results suggest, then it's possible that these individuals would exhibit similar neural patterns to those in the PST condition, who were also less stressed, in the aggregate (as opposed to trial by trial). Within DMT

dyads, 81 statistically significant whole brain connections were found (connections presented in Figure 10). Regions with the most meaningful connectivity, or hubs defined by five or more significant connections, were as follows: Posterior Cingulate Cortex (R) and Transverse Temporal Cortex (L, Figure 10). Just as in the previous analysis, fewer hubs were identified, which is not surprising given that these individuals were not working with one another.

The classification rate from the SVM model was .53, meaning only 53% of participants within these groups could be classified to their respective conditions. After permutation testing, classification was confirmed to be unreliable in classifying between DMT actors and PST dyad members ($p > .05$). Overall this suggests that DMT actors and those in the PST dyad condition were processing performance feedback in a similar manner, at least in the aggregate (i.e., across the entirety of the task), despite DMT actors initially experiencing SBS. This is supportive of the notion that SBS contagion occurs rapidly during the beginning of the task, such that towards the middle and end of the task DMT actors were processing feedback in a manner that, at least with respect to these MVPA data driven analyses, was similar to PST dyads.

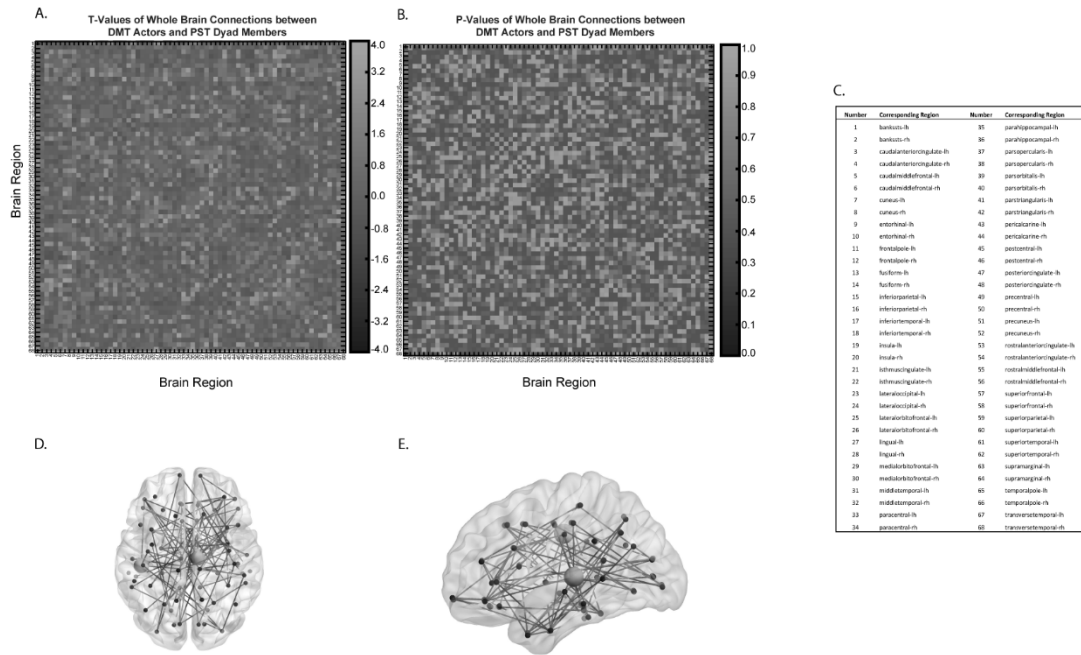


Figure 10 A) PLV t-test values between DMT actors and PST dyad members. Black shades indicate negative correlations, grey shades indicate positive correlations. B) PLV significant values between DMT actors and PST dyad members. Black shades indicate $p < .05$. C) Corresponding neural regions for matrices A and B. D) Neural distribution of significant hubs and connections between DMT actors and PST dyad members; horizontal plane. Larger hubs indicate increased connectivity with other regions. E) Neural distribution of significant hubs and connections between DMT actors and PST dyad members; sagittal plane. Larger hubs indicate increased connectivity with other regions.

Chapter 6

DISCUSSION

Overall, findings suggest SBS contagion can occur within female dyads working in problem solving contexts and has different consequences on performance for each member of the dyad. While working together on a math task, DMT partners performed worse over time whereas DMT actors, i.e., those placed directly in a SBS context, performed better and comparable to dyads working in SBS neutral contexts. Furthermore, both DMT actors and partners exhibited neural indices indicative of stress early in the interaction. While DMT partners exhibited sustained higher levels of vACC power over the course of the task, DMT actors evoked vACC power that, while initially high, steadily decreased over time. Both levels were greater than that found in SBS-neutral contexts, suggesting that SBS contexts were stressful for both DMT actors and their partners. Importantly, DMT partners showed evidence of “catching” this initial stress response from the threatened actor; emotion saliency network connectivity to feedback from DMT actors on trial n predicted emotion saliency network connectivity to feedback in their partners on trial $n + 1$ over the course of the task. “Catching” this initial stress in turn had direct ramifications for DMT partners’ performance. DMT partners underperformed on the math task over time to the extent they exhibited increased connectivity in the emotion saliency network to performance feedback. This effect was also most pronounced towards the beginning of the task, implicating this time period as particularly critical with respect to contagion effects. Importantly, these relationships were not evident within PST dyad members interacting in stereotype neutral contexts.

Follow up MVPA results provided further evidence for SBS contagion. Both DMT and PST actors and partners could not be classified with reliable accuracy within their respective dyads, suggesting partners were processing performance feedback similarly to actors within both contexts (understandably, as these dyads were working together on the problem solving task). Importantly, while data driven analyses within both DMT and PST dyads revealed hubs associated with executive function and attentional control, e.g., Post Central Gyrus, Rostral Middle Frontal Cortex, and Temporal Pole (Alvarez & Emory, 2006; Raye et al., 2007; Hopfinger, Buonocore, & Mangun, 2000), only DMT dyads yielded a hub, the vACC, that is both heavily implicated in stress responses in general and a hub in a priori based emotion saliency network analyses. In other words, these results suggest that DMT actors and partners were engaged in more arousal-oriented emotional processing of performance feedback in line with a priori-based emotion saliency network analyses. It should be noted that the insula was also identified within PST dyads, which is a region often associated with emotional processing and awareness in general. However, this region also plays a key role in attentional allocation and functionality may largely depend on whether activity stems from anterior or posterior aspects of the region (Nelson et al., 2010). EEG does not provide us with the spatial resolution to distinguish between which aspect of insula was implicated in these analyses, thus future research utilizing fMRI methods would be necessary to address these issues.

MVPA analyses were able to distinguish between DMT and PST actors and partners. In addition to analyses yielding fewer neural hubs (understandably, as these groups were not working together on the interactive math task), DMT and PST partners were found to be statistically distinguishable from one another with high

accuracy, despite these women being in the same condition (instruction-wise). Hubs associated with arousal-oriented emotional processing and executive function accurately classified/distinguished between these two groups, suggesting that DMT partners were experiencing greater emotion and arousal as a function of the threatened partner they were interacting with compared to PST partners and their non-threatened partner. Conversely, and perhaps surprisingly, DMT actors and PST dyad members were indistinguishable from one another. While DMT actors demonstrated heightened vACC activity and network connectivity than members of PST dyads initially in a priori analyses, data-driven MVPA analyses, which collapse across feedback related EEG activity elicited throughout the task, suggest DMT actors were more like members of PST dyads. Based on a priori analyses these similarities were likely more prevalent towards the middle and end of the task. This would be expected if DMT actors initially transferred their stress to their partners and experienced less stress over time as a result. This would be similar to the experience had by PST dyads overall (which a priori analyses also allude to). While these initial results are promising, future research utilizing more precise source localization methods, e.g., fMRI, would be necessary to corroborate these findings.

Findings from this study provide further insight on the dynamic relationship between two individuals performing in domains where their common identity is devalued. Although it seems conceivable that the performance of both DMT actors and partners would suffer when solving problems together in a negatively stereotyped domain, results provide further support for the notion that non-threatened partners help buffer initially threatened actors from the deleterious consequences of SBS over time, at their own expense. These findings are consistent with past work showing that the

presence of a female role model or competent female partner alleviates performance decrements otherwise typically evident in stereotype threatening contexts (Marx and Roman 2002; McIntyre et al., 2005; Thorson et al., 2019). Results expand upon this work in several ways. Most notably, by demonstrating that the transference of an individual's stress response on to their partners (evidenced here as DMT actor's decreased vACC activity over time, emotion saliency network connectivity predicting partner's emotion saliency network connectivity, and similar MVPA based neural profiles exhibited by DMT actors and partners during feedback processing) may be one important factor in buffering women from SBS during dyadic problem solving interactions, particularly during initial stages of the interaction. Conversely, like past work demonstrating that increased emotional processing of feedback in SBS contexts has a negative impact on individuals' performance when alone (Forbes et al., 2015; Forbes et al., 2018), findings from this study demonstrate that this effect extends to partners in a dyadic interaction, providing a potential mechanism for underperformance effects among these individuals in group problem solving contexts moving forward.

Our findings also add to the stress and emotion contagion literature in several important ways. Past work on stress and emotion contagion describes this phenomenon as occurring within minutes of an interaction with behavioral mimicry, HRV, and cortisol being common quantitative markers. This suggests that interpretations of the contagion phenomenon have been constrained by the limits of the measures used to index it, which is particularly relevant in this case given that measures such as HRV and cortisol are either collected on the order of seconds or minutes and takes tens of minutes to manifest in the case of cortisol specifically (in

addition to being contingent on a wide number of factors, e.g., time of day; Waters et al., 2017; Dimitroff et al., 2017; Schoebi, 2008; West, et al., 2017). Using neuroscience methodologies, our results provide novel insight into how contagion manifests on the order of milliseconds, a much more rapid timescale than previously assumed, to affect performance accordingly; 500ms samples of neural network connectivity elicited in response to performance feedback reliably predicted performance on the following trial for DMT partners specifically. Moreover, the design of the present study provides a novel yet realistic platform to examine emotion contagion phenomena via EEG or fMRI methodology in future studies. By using iPads it was possible to capture simultaneous EEG activity in a controlled manner while still allowing participants to have a real time face to face interaction. This design also provides implications for contagion hypotheses specific to the mimicry and proximity literature. Because participants only communicated through an iPad webcam, participants were only able to view their partners face and hear their voice through the webcam during the interaction. This suggests that vocal patterns and facial expressions may have played an integral role in facilitating contagion effects, bolstering previous research (Hatfield, Cacioppo, & Rapson, 1993; Neumann & Strack, 2000).

Specific hypotheses were not made for frequency bands but nonetheless findings were consistent with past literature. After correcting for multiple comparisons, effects were specific to the theta band for emotional network connectivity and the gamma band for vACC activation to negative performance feedback. Both frequency bands have been linked to stress and emotion-oriented processes. For instance, while theta frequencies have been linked to valence-oriented emotional responses to images and faces (Aftanas et al, 2001; Başar, Güntekin, &

Öniz, 2006; Güntekin & Başar, 2009), gamma frequencies have been utilized to examine levels of arousal elicited during the processing of emotional images (Balconi & Mazza, 2009, Balconi et. al 2008, Keil et al. 2001). These frequency bands also often covary with one another and represent different aspects of excitatory neural activity (Buzsaki, 2006). Consistent with this, the theta, beta and gamma bands for our specific measures of interest were all correlated with one another ($p's < .001$).

Regarding limitations of the study, it is important to note that when considering EEG data and the spatial limitations associated with the methodology, conclusions based on precise brain locations should always be interpreted with caution. Nevertheless, this study utilized a high density electrode array and an advanced source Bayesian analytic approach. This Bayesian analytic approach includes dSPM inverse operators confining analyses to regions closer to the cortical surface. With this approach it is possible to make accurate assumptions about specific brain region contributions (Cohen, 2014). Moreover, regions in a priori networks were identified in a separate unbiased data-driven MVPA analysis that utilizes different source localization procedures, providing consistency across source localization approaches. Results should, however, be replicated and expanded upon in future fMRI studies, although given the temporal constraints of fMRI methodologies with respect to findings in this study (i.e., these effects may occur on the order of milliseconds), this approach could be problematic as well.

Future research also should address how the experience and occurrence of SBS contagion manifests between male-female dyads working in STEM settings. Past research suggests that at the individual level, the mere presence of men can exacerbate SBS effects (Inzlicht & Ben-Zeev, 2000). Given that emotional contagion is also

dependent to an extent on perceived similarity, in-group status and affiliation, it's possible that SBS contagion does not occur at all between male- female dyads. Consistent with this, initial evidence suggests that women experiencing an identity threat do not behaviorally engage and physiologically synchronize (operationalized as pre-ejection period volumes over 30 second intervals) with male partners compared to female partners, and they still underperform accordingly (Thorson et al., 2019). This suggests SBS contagion may not occur among male-female dyads, nor would male partners buffer women experiencing SBS from the deleterious consequences normally evident among individuals in SBS contexts.

When women review for an exam or complete a group project in STEM contexts, domains in which they are negatively stereotyped, they often work together to promote individual success and foster solidarity. Although these interactions are perceived to be beneficial for all, depending on sensitivities of some women to negative group stereotypes, these interactions may do more harm than good for some of these women. Ironically, this harm may be engendered in part by too much solidarity; two individuals identifying and empathizing with one another, and subsequently neurally synchronizing with one another to the point where they share in the stress experience. While this helps those initially experiencing the most stress, it comes at the direct cost of those otherwise not stressed. Although the findings in this study provide novel insight into the potential pitfalls of women working together in SBS contexts, they also provide insight into ways that can potentially reverse these effects. When women in stereotype neutral contexts performed identical tasks to those in identity threatening contexts, SBS contagion and subsequent performance decrements were non-existent. Thus, one way to potentially reverse the deleterious

consequences of SBS situations is to strive to maintain an identity safe environment. This could be as simple as framing STEM activities as problem solving tasks and keeping gender primes as minimal as possible; simple albeit effective manipulations. Overall, findings provide a more nuanced understanding of the contagion process while also providing a better understanding of a heretofore largely unexamined question in the literature: how social identity threats and SBS manifest in dyadic interactions to have paradoxical effects on performance. More importantly, findings provide further insight into the many ways the gender gap in STEM domains can be perpetuated but also one day nullified.

REFERENCES

Aftanas, L. I., Varlamov, A. A., Pavlov, S. V., Makhnev, V. P., & Reva, N. V. (2001). Affective picture processing: event-related synchronization within individually defined human theta band is modulated by valence dimension. *Neuroscience letters*, *303*(2), 115-118.

Alvarez, J. A., & Emory, E. (2006). Executive function and the frontal lobes: a meta-analytic review. *Neuropsychology review*, *16*(1), 17-42.

Attal, Y., & Schwartz, D. (2013). Assessment of subcortical source localization using deep brain activity imaging model with minimum norm operators: a MEG study. *PLoS One*, *8*(3), e59856.

Axmacher, N., Henseler, M. M., Jensen, O., Weinreich, I., Elger, C. E., & Fell, J. (2010). Cross-frequency coupling supports multi-item working memory in the human hippocampus. *Proceedings of the National Academy of Sciences*, *107*(7), 3228-3233.

Balconi, M., & Lucchiari, C. (2008). Consciousness and arousal effects on emotional face processing as revealed by brain oscillations. A gamma band analysis. *International Journal of Psychophysiology*, *67*(1), 41-46.

Balconi, M., & Mazza, G. (2009). Brain oscillations and BIS/BAS (behavioral inhibition/activation system) effects on processing masked emotional cues.: ERS/ERD and coherence measures of alpha band. *International Journal of Psychophysiology*, *74*(2), 158-165.

Ballinger, G. A. (2004). Using generalized estimating equations for longitudinal data analysis. *Organizational research methods*, *7*(2), 127-150.

Barsade, S. G. (2002). The ripple effect: Emotional contagion and its influence on group behavior. *Administrative Science Quarterly*, 47(4), 644-675.

Başar, E., Güntekin, B., & Öviz, A. (2006). Principles of oscillatory brain dynamics and a treatise of recognition of faces and facial expressions. *Progress in brain research*, 159, 43-62.

Bassett, D. S., & Sporns, O. (2017). Network neuroscience. *Nature neuroscience*, 20(3), 353.

Beasley, M. A., & Fischer, M. J. (2012). Why they leave: The impact of stereotype threat on the attrition of women and minorities from science, math and engineering majors. *Social Psychology of Education*, 15(4), 427-448.

Benjamini, Y., & Hochberg, Y. (1995). Controlling the false discovery rate: a practical and powerful approach to multiple testing. *Journal of the royal statistical society. Series B (Methodological)*, 289-300.

Bhattacharya, J. (2017). Cognitive neuroscience: synchronizing brains in the classroom. *Current Biology*, 27(9), R346-R348.

Blascovich, J., Spencer, S.J., Quinn, D., Steele, C. (2001). African Americans and high blood pressure: the role of stereotype threat. *Psychological Science*, 12(3), 225–9.

Brooks, S. J., Savov, V., Allzén, E., Benedict, C., Fredriksson, R., & Schiöth, H. B. (2012). Exposure to subliminal arousing stimuli induces robust activation in the amygdala, hippocampus, anterior cingulate, insular cortex and primary visual cortex: a systematic meta-analysis of fMRI studies. *NeuroImage*, 59(3), 2962-2973.

Bush, G., Luu, P., & Posner, M. I. (2000). Cognitive and emotional influences in anterior cingulate cortex. *Trends in cognitive sciences*, 4(6), 215-222.

- Buzsaki, G. (2006). *Rhythms of the Brain*. Oxford University Press.
- Chen, G., Chen, G., Xie, C., & Li, S. J. (2011). Negative functional connectivity and its dependence on the shortest path length of positive network in the resting-state human brain. *Brain connectivity, 1*(3), 195-206.
- Chen, H., Duan, X., Liu, F., Lu, F., Ma, X., Zhang, Y., ... & Chen, H. (2016). Multivariate classification of autism spectrum disorder using frequency-specific resting-state functional connectivity—a multi-center study. *Progress in Neuro-Psychopharmacology and Biological Psychiatry, 64*, 1-9.
- Chen, J. L., Ros, T., & Gruzelier, J. H. (2013). Dynamic changes of ICA-derived EEG functional connectivity in the resting state. *Human brain mapping, 34*(4), 852-868.
- Cheryan, S., Siy, J. O., Vichayapai, M., Drury, B. J., & Kim, S. (2011). Do female and male role models who embody STEM stereotypes hinder women's anticipated success in STEM?. *Social Psychological and Personality Science, 2*(6), 656-664.
- Cohen, G. L., & Garcia, J. (2005). "I am us": negative stereotypes as collective threats. *Journal of personality and social psychology, 89*(4), 566.
- Cohen, J. D., Perlstein, W. M., Braver, T. S., Nystrom, L. E., Noll, D. C., Jonides, J., & Smith, E. E. (1997). Temporal dynamics of brain activation during a working memory task. *Nature, 386*(6625), 604.
- Cohen, M. X. (2014). *Analyzing neural time series data: theory and practice*. MIT press.
- Corbetta, M., & Shulman, G. L. (2002). Control of goal-directed and stimulus-driven attention in the brain. *Nature reviews neuroscience, 3*(3), 201.

Dale, A. M., Fischl, B., & Sereno, M. I. (1999). Cortical surface-based analysis: I. Segmentation and surface reconstruction. *Neuroimage*, 9(2), 179-194.

Dale, A. M., Liu, A. K., Fischl, B. R., Buckner, R. L., Belliveau, J. W., Lewine, J. D., & Halgren, E. (2000). Dynamic statistical parametric mapping: Combining fMRI and MEG for high-resolution imaging of cortical activity. *Neuron*, 26(1), 55-67.

Dasgupta, N., Scircle, M. M., & Hunsinger, M. (2015). Female peers in small work groups enhance women's motivation, verbal participation, and career aspirations in engineering. *Proceedings of the National Academy of Sciences*, 201422822.

Deaux, K., & Lewis, L. L. (1984). Structure of gender stereotypes: Interrelationships among components and gender label. *Journal of personality and Social Psychology*, 46(5), 991.

Decety, J., Norman, G. J., Berntson, G. G., & Cacioppo, J. T. (2012). A neurobehavioral evolutionary perspective on the mechanisms underlying empathy. *Progress in neurobiology*, 98(1), 38-48.

Desikan, R. S., Ségonne, F., Fischl, B., Quinn, B. T., Dickerson, B. C., Blacker, D., ... & Albert, M. S. (2006). An automated labeling system for subdividing the human cerebral cortex on MRI scans into gyral based regions of interest. *Neuroimage*, 31(3), 968-980.

Dikker, S., Silbert, L. J., Hasson, U., & Zevin, J. D. (2014). On the same wavelength: predictable language enhances speaker–listener brain-to-brain synchrony in posterior superior temporal gyrus. *Journal of Neuroscience*, 34(18), 6267-6272.

Dikker, S., Wan, L., Davidesco, I., Kaggen, L., Oostrik, M., McClintock, J., ... & Poeppel, D. (2017). Brain-to-brain synchrony tracks real-world dynamic group interactions in the classroom. *Current Biology*, 27(9), 1375-1380.

Dimitroff, S. J., Kardan, O., Necka, E. A., Decety, J., Berman, M. G., & Norman, G. J. (2017). Physiological dynamics of stress contagion. *Scientific reports*, 7(1), 6168.

Dipoppa, M., & Gutkin, B. S. (2013). Flexible frequency control of cortical oscillations enables computations required for working memory. *Proceedings of the National Academy of Sciences*, 110(31), 12828-12833.

Dosenbach, N. U., Fair, D. A., Miezin, F. M., Cohen, A. L., Wenger, K. K., Dosenbach, R. A., ... & Schlaggar, B. L. (2007). Distinct brain networks for adaptive and stable task control in humans. *Proceedings of the National Academy of Sciences*, 104(26), 11073-11078.

Dumas, G., Nadel, J., Soussignan, R., Martinerie, J., & Garnero, L. (2010). Inter-brain synchronization during social interaction. *PloS one*, 5(8), e12166.

Etkin, A., Egner, T., & Kalisch, R. (2011). Emotional processing in anterior cingulate and medial prefrontal cortex. *Trends in cognitive sciences*, 15(2), 85-93.

Fagot, B. I. (1977). Consequences of moderate cross-gender behavior in preschool children. *Child Development*, 902-907.

Figley, C. R. (2013). *Compassion fatigue: Coping with secondary traumatic stress disorder in those who treat the traumatized*. Routledge.

Fitzmaurice, G. M., Laird, N. M., & Rotnitzky, A. G. (1993). Regression models for discrete longitudinal responses. *Statistical Science*, 284-299.

Fitzmaurice, G. M., Laird, N. M., & Ware, J. H. (2012). *Applied longitudinal analysis* (Vol. 998). John Wiley & Sons.

Forbes, C. E., & Leitner, J. B. (2014). Stereotype threat engenders neural attentional bias toward negative feedback to undermine performance. *Biological psychology, 102*, 98-107.

Forbes, C. E., Amey, R., Magerman, A. B., Duran, K., & Liu, M. (2018). Stereotype-based stressors facilitate emotional memory neural network connectivity and encoding of negative information to degrade math self-perceptions among women. *Social cognitive and affective neuroscience, 1*, 22.

Forbes, C. E., Duran, K. A., Leitner, J. B., & Magerman, A. (2015). Stereotype threatening contexts enhance encoding of negative feedback to engender underperformance and anxiety. *Social Cognition, 33*(6), 605-625.

Gonzales, P. M., Blanton, H., & Williams, K. J. (2002). The effects of stereotype threat and double-minority status on the test performance of Latino women. *Personality and social psychology bulletin, 28*(5), 659-670.

Gramfort, A., Luessi, M., Larson, E., Engemann, D. A., Strohmeier, D., Brodbeck, C., ... & Hämäläinen, M. (2013). MEG and EEG data analysis with MNE-Python. *Frontiers in neuroscience, 7*, 267.

Gramfort, A., Luessi, M., Larson, E., Engemann, D. A., Strohmeier, D., Brodbeck, C., ... & Hämäläinen, M. S. (2014). MNE software for processing MEG and EEG data. *Neuroimage, 86*, 446-460.

Güntekin, B., & Başar, E. (2009). Facial affect manifested by multiple oscillations. *International Journal of Psychophysiology, 71*(1), 31-36.

Hamalainen, M. S., & Sarvas, J. (1989). Realistic conductivity geometry model of the human head for interpretation of neuromagnetic data. *IEEE transactions on biomedical engineering*, *36*(2), 165-171.

Hamalainen, M. S., & Sarvas, J. (1989). Realistic conductivity geometry model of the human head for interpretation of neuromagnetic data. *IEEE transactions on biomedical engineering*, *36*(2), 165-171.

Hampshire, A., Chamberlain, S. R., Monti, M. M., Duncan, J., & Owen, A. M. (2010). The role of the right inferior frontal gyrus: inhibition and attentional control. *Neuroimage*, *50*(3), 1313-1319.

Harding, I. H., Yücel, M., Harrison, B. J., Pantelis, C., & Breakspear, M. (2015). Effective connectivity within the frontoparietal control network differentiates cognitive control and working memory. *Neuroimage*, *106*, 144-153.

Harenski, C. L., & Hamann, S. (2006). Neural correlates of regulating negative emotions related to moral violations. *Neuroimage*, *30*(1), 313-324.

Hatfield, E., Cacioppo, J. T., & Rapson, R. L. (1993). Emotional contagion. *Current directions in psychological science*, *2*(3), 96-100.

Hopfinger, J. B., Buonocore, M. H., & Mangun, G. R. (2000). The neural mechanisms of top-down attentional control. *Nature neuroscience*, *3*(3), 284.

Inzlicht, M., & Ben-Zeev, T. (2000). A threatening intellectual environment: Why females are susceptible to experiencing problem-solving deficits in the presence of males. *Psychological Science*, *11*(5), 365-371.

Jahng, J., Kralik, J. D., Hwang, D. U., & Jeong, J. (2017). Neural dynamics of two players when using nonverbal cues to gauge intentions to cooperate during the Prisoner's Dilemma Game. *NeuroImage*, *157*, 263-274.

Keil, A., Müller, M. M., Gruber, T., Wienbruch, C., Stolarova, M., & Elbert, T. (2001). Effects of emotional arousal in the cerebral hemispheres: a study of oscillatory brain activity and event-related potentials. *Clinical neurophysiology*, *112*(11), 2057-2068.

Kim, M. J., Loucks, R. A., Palmer, A. L., Brown, A. C., Solomon, K. M., Marchante, A. N., & Whalen, P. J. (2011). The structural and functional connectivity of the amygdala: from normal emotion to pathological anxiety. *Behavioural brain research*, *223*(2), 403-410.

Krendl, A. C., Richeson, J. A., Kelley, W. M., & Heatherton, T. F. (2008). The negative consequences of threat: A functional magnetic resonance imaging investigation of the neural mechanisms underlying women's underperformance in math. *Psychological Science*, *19*(2), 168-175.

LaBar, K. S., & Cabeza, R. (2006). Cognitive neuroscience of emotional memory. *Nature Reviews Neuroscience*, *7*(1), 54.

Lachaux, J. P., Rodriguez, E., Le Van Quyen, M., Lutz, A., Martinerie, J., & Varela, F. J. (2000). Studying single-trials of phase synchronous activity in the brain. *International Journal of Bifurcation and Chaos*, *10*(10), 2429-2439.

Liang, K. Y., & Zeger, S. L. (1986). Longitudinal data analysis using generalized linear models. *Biometrika*, *73*(1), 13-22.

Lin, F., Belliveau, J. W., Dale, A. M., & Hämäläinen, M. S. (2006). Distributed current estimates using cortical orientation constraints. *Human Brain Mapping*, *27*(1), 1-13.

Liu, F., Guo, W., Yu, D., Gao, Q., Gao, K., Xue, Z., ... & Zhao, J. (2012). Classification of different therapeutic responses of major depressive disorder with

multivariate pattern analysis method based on structural MR scans. *PloS one*, 7(7), e40968.

Liu, M., Amey, R. C., & Forbes, C. E. (2017). On the Role of Situational Stressors in the Disruption of Global Neural Network Stability during Problem Solving. *Journal of cognitive neuroscience*, 29(12), 2037-2053.

Liu, M., Kuo, C., & Chiu, A. W. (2011). Statistical threshold for nonlinear granger causality in motor intention analysis. *2011 Annual International Conference of the IEEE Engineering in Medicine and Biology Society*, 5036-5039.

Liu, M., Kuo, C., & Chiu, A. W. (2013). Non-linear Granger causality and its frequency decomposition in decoding human upper limb movement intentions. *International Journal of Biomedical Engineering and Technology* 34, 12(1), 1-25.

Lockwood, P., & Kunda, Z. (1997). Superstars and me: Predicting the impact of role models on the self. *Journal of personality and social psychology*, 73(1), 91.

Mahmoudi, A., Takerkart, S., Regragui, F., Boussaoud, D., & Brovelli, A. (2012). Multivoxel pattern analysis for fMRI data: a review. *Computational and mathematical methods in medicine*, 2012.

Mangels, J. A., Good, C., Whiteman, R. C., Maniscalco, B., & Dweck, C. S. (2011). Emotion blocks the path to learning under stereotype threat. *Social cognitive and affective neuroscience*, 7(2), 230-241.

Marx, D. M., & Goff, P. A. (2005). Clearing the air: The effect of experimenter race on target's test performance and subjective experience. *British Journal of Social Psychology*, 44(4), 645-657.

Marx, D. M., & Roman, J. S. (2002). Female role models: Protecting women's math test performance. *Personality and Social Psychology Bulletin*, 28(9), 1183-1193.

McIntyre, R. B., Lord, C. G., Gresky, D. M., Ten Eyck, L. L., Frye, G. J., & Bond Jr, C. F. (2005). A social impact trend in the effects of role models on alleviating women's mathematics stereotype threat. *Current Research in Social Psychology*, 10(9), 116-36.

Mišić, B., & Sporns, O. (2016). From regions to connections and networks: new bridges between brain and behavior. *Current opinion in neurobiology*, 40, 1-7.

Murphy, M. C., Steele, C. M., & Gross, J. J. (2007). Signaling threat: How situational cues affect women in math, science, and engineering settings. *Psychological Science*, 18(10), 879-885.

Murty, V. P., Ritchey, M., Adcock, R. A., & LaBar, K. S. (2010). fMRI studies of successful emotional memory encoding: A quantitative meta-analysis. *Neuropsychologia*, 48(12), 3459-3469.

Nelson, S. M., Dosenbach, N. U., Cohen, A. L., Wheeler, M. E., Schlaggar, B. L., & Petersen, S. E. (2010). Role of the anterior insula in task-level control and focal attention. *Brain structure and function*, 214(5-6), 669-680.

Neumann, R., & Strack, F. (2000). "Mood contagion": the automatic transfer of mood between persons. *Journal of personality and social psychology*, 79(2), 211.

Nolan, H., Whelan, R., & Reilly, R. B. (2010). FASTER: fully automated statistical thresholding for EEG artifact rejection. *Journal of neuroscience methods*, 192(1), 152-162.

Nolte, T., Bolling, D. Z., Hudac, C., Fonagy, P., Mayes, L. C., & Pelphrey, K. A. (2013). Brain mechanisms underlying the impact of attachment-related stress on social cognition. *Frontiers in human neuroscience*, 7, 816.

Nummenmaa, L., & Saarimäki, H. (2017). Emotions as discrete patterns of systemic activity. *Neuroscience letters*.

Nummenmaa, L., Hirvonen, J., Parkkola, R., & Hietanen, J. K. (2008). Is emotional contagion special? An fMRI study on neural systems for affective and cognitive empathy. *Neuroimage*, 43(3), 571-580.

Osborne, J.W. (2006). Gender, stereotype and threat anxiety: Psychophysiological and cognitive evidence. *Journal of Research in Educational Psychology*, 8, 109–38.

Osborne, J.W. (2007). Linking stereotype threat and anxiety. *Educational Psychology*, 27(1), 135–54.

Park, H. J., & Friston, K. (2013). Structural and functional brain networks: from connections to cognition. *Science*, 342(6158), 1238411.

Petersen, S. E., & Sporns, O. (2015). Brain networks and cognitive architectures. *Neuron*, 88(1), 207-219.

Pintzinger, N. M., Pfabigan, D. M., Pfau, L., Kryspin-Exner, I., & Lamm, C. (2017). Temperament differentially influences early information processing in men and women: preliminary electrophysiological evidence of attentional biases in healthy individuals. *Biological psychology*, 122, 69-79.

Raye, C. L., Johnson, M. K., Mitchell, K. J., Greene, E. J., & Johnson, M. R. (2007). Refreshing: A minimal executive function. *Cortex*, 43(1), 135-145.

Rubinov, M., & Sporns, O. (2011). Weight-conserving characterization of complex functional brain networks. *Neuroimage*, *56*(4), 2068-2079.

Rudie, J. D., Brown, J. A., Beck-Pancer, D., Hernandez, L. M., Dennis, E. L., Thompson, P. M., ... & Dapretto, M. (2013). Altered functional and structural brain network organization in autism. *NeuroImage: clinical*, *2*, 79-94.

Rudman, L. A., & Fairchild, K. (2004). Reactions to counterstereotypic behavior: the role of backlash in cultural stereotype maintenance. *Journal of personality and social psychology*, *87*(2), 157.

Schmader, T., Forbes, C. E., Zhang, S., & Berry Mendes, W. (2009). A metacognitive perspective on the cognitive deficits experienced in intellectually threatening environments. *Personality and Social Psychology Bulletin*, *35*(5), 584-596.

Schmader, T., Johns, M., & Forbes, C. (2008). An integrated process model of stereotype threat effects on performance. *Psychological review*, *115*(2), 336.

Schoebi, D. (2008). The coregulation of daily affect in marital relationships. *Journal of Family Psychology*, *22*(4), 595.

Schwarz, A. J., & McGonigle, J. (2011). Negative edges and soft thresholding in complex network analysis of resting state functional connectivity data. *Neuroimage*, *55*(3), 1132-1146.

Seeley, W. W., Menon, V., Schatzberg, A. F., Keller, J., Glover, G. H., Kenna, H., ... & Greicius, M. D. (2007). Dissociable intrinsic connectivity networks for salience processing and executive control. *Journal of Neuroscience*, *27*(9), 2349-2356.

Sekaquaptewa, D., & Thompson, M. (2003). Solo status, stereotype threat, and performance expectancies: Their effects on women's performance. *Journal of Experimental Social Psychology, 39*(1), 68-74.

Shih, M., Pittinsky, T. L., & Ambady, N. (1999). Stereotype susceptibility: Identity salience and shifts in quantitative performance. *Psychological science, 10*(1), 80-83.

Singh, A. K., & Phillips, S. (2010). Hierarchical control of false discovery rate for phase locking measures of EEG synchrony. *NeuroImage, 50*(1), 40-47.

Sporns, O. (2011). *Networks of the Brain*. MIT press.

Sporns, O., & Betzel, R. F. (2016). Modular brain networks. *Annual review of psychology, 67*, 613-640.

Steele, C. M., & Aronson, J. (1995). Stereotype threat and the intellectual test performance of African Americans. *Journal of personality and social psychology, 69*(5), 797.

Steele, C. M., Spencer, S. J., & Aronson, J. (2002). Contending with group image: The psychology of stereotype and social identity threat. In *Advances in experimental social psychology* (Vol. 34, pp. 379-440). Academic Press.

Stout, J. G., Dasgupta, N., Hunsinger, M., & McManus, M. A. (2011). STEMing the tide: using ingroup experts to inoculate women's self-concept in science, technology, engineering, and mathematics (STEM). *Journal of personality and social psychology, 100*(2), 255.

Thompson, W. H., & Fransson, P. (2017). Spatial confluence of psychological and anatomical network constructs in the human brain revealed by a mass meta-analysis of fMRI activation. *Scientific reports, 7*, 44259.

Thorson, K. R., & West, T. V. (2018). Physiological linkage to an interaction partner is negatively associated with stability in sympathetic nervous system responding. *Biological psychology, 138*, 91-95.

Thorson, K. R., Forbes, C. E., Magerman, A. B., & West, T. V. (2019). Under threat but engaged: Stereotype threat leads women to engage with female but not male partners in math. *Contemporary Educational Psychology*.

Townsend, S.S.M., Major, B., Gangi, C.E., Mendes, W.B. (2011). From “In the Air” to “Under the Skin”: cortisol responses to social identity threat. *Personality & Social Psychology Bulletin, 37*(2), 151–64.

Viviani, R. (2013). Emotion regulation, attention to emotion, and the ventral attentional network. *Frontiers in human neuroscience, 7*, 746.

Vuilleumier, P. (2005). How brains beware: neural mechanisms of emotional attention. *Trends in cognitive sciences, 9*(12), 585-594.

Waters, S. F., West, T. V., & Mendes, W. B. (2014). Stress contagion: Physiological covariation between mothers and infants. *Psychological science, 25*(4), 934-942.

Waters, S. F., West, T. V., Karnilowicz, H. R., & Mendes, W. B. (2017). Affect contagion between mothers and infants: Examining valence and touch. *Journal of Experimental Psychology: General, 146*(7), 1043.

West, T. V. (2013). Repeated measures with dyads. In *The Oxford handbook of close relationships*.

West, T. V., Koslov, K., Page-Gould, E., Major, B., & Mendes, W. B. (2017). Contagious anxiety: anxious European Americans can transmit their physiological reactivity to African Americans. *Psychological science, 28*(12), 1796-1806.

Zhang, Q., Wu, Q., Zhu, H., He, L., Huang, H., Zhang, J., & Zhang, W.
(2016). Multimodal MRI-based classification of trauma survivors with and without
post-traumatic stress disorder. *Frontiers in neuroscience*, *10*, 292.

Appendix A

SUPPLEMENTARY ANALYSES

Effects of SBSC on Partner's Performance. Emotion and stress perception network connectivity to both positive and negative performance feedback was included in the model to remain consistent with previous analyses given the novel dyadic context. However, Considering evidence from previous literature suggests SBS contexts prompt negative performance feedback to be processed differently than positive performance feedback (Forbes & Leitner, 2014; Forbes et al., 2015; Forbes et al., 2018; Mangels et al. 2011), we could expect emotion and stress perception network connectivity effects on performance to be specific to negative performance feedback for participants experiencing SBS. This resulted in an over time, factorial model that included condition, emotion and stress perception network connectivity to all performance feedback, and time as predictors. This initial model yielded a significant two-way interaction between condition and time (Wald $\chi^2(2) = 9.94, p < .01$). Simple effects revealed that DMT partners performance decreased over the course of the task relative to levels of emotion and stress perception network connectivity ($b = -.005$, Wald $\chi^2(1) = 5.001$, 95% CI [-0.009, -0.001], $SE = .0022$, $p < .03$). No other effects for time were found with any other group (p 's $> .15$). A Marginal three-way interaction between condition, time, and emotion and stress perception network connectivity to performance feedback was observed ($p = .09$), however, no two-way interactions were qualified by the three-way marginal interaction.

Supplementary Analysis Tables

Table A.1 Hypothesis 1: SBSC Impacts Performance Interaction Breakdown

Table 1
Hypothesis 1: SBSC impacts performance

Interaction Breakdown	<i>b</i>	<i>SE</i>	<i>LLCI</i>	<i>ULCI</i>	<i>Wald</i>	<i>df</i>	<i>p</i>
The simple slope of time for the DMT partner	-0.005	0.002	-0.009	-0.002	7.452	1.000	0.006
The simple slope of time for the DMT actor	0.003	0.002	-0.001	0.007	2.569	1.000	0.109
The simple slope of time for the PST dyad member	0.001	0.002	-0.003	0.004	0.128	1.000	0.720

Table A.2 Hypothesis 1: SBSC Impacts Performance Simple Contrasts

Table 2
Hypothesis 1: SBSC impacts performance

Simple Contrasts	<i>Mean Difference</i>	<i>SE</i>	<i>LLCI</i>	<i>ULCI</i>	<i>df</i>	<i>p</i>
DMT partner vs. DMT actor performance at the beginning of the task	0.080	0.026	0.030	0.130	1.000	0.002
DMT partner vs. PST member performance at the beginning of the task	0.060	0.029	0.004	0.120	1.000	0.034
DMT actor vs. PST dyad member performance at the beginning of the task	-0.020	0.028	-0.070	0.040	1.000	0.491
DMT partner vs. DMT actor performance at the end of the task	-0.070	0.025	-0.120	-0.020	1.000	0.004
DMT partner vs. PST member performance at the end of the task	-0.050	0.027	-0.100	0.010	1.000	0.089
DMT actor vs. PST member performance at the end of the task	0.030	0.028	-0.030	0.080	1.000	0.348

Table A.3 Hypothesis 2: SBSC Promotes Changes in Neural Network Activity
Interaction Breakdown

Table 3

Hypothesis 2: SBSC promotes changes in neural activity

Interaction Breakdown	<i>b</i>	<i>SE</i>	<i>LLCI</i>	<i>ULCI</i>	<i>Wald</i>	<i>df</i>	<i>p</i>
Simple 2-way condition x time interaction for positive feedback	NA	NA	NA	NA	0.366	2.000	0.833
Simple 2-way condition x time interaction for negative feedback	NA	NA	NA	NA	9.746	2.000	0.008
The simple slope of time for the DMT partner and negative feedback	0.000	0.001	-0.002	0.002	0.065	1.000	0.798
The simple slope of time for the DMT actor and negative feedback	-0.005	0.001	-0.007	-0.002	16.696	1.000	0.000
The simple slope of time for the PST dyad member and negative feedback	-0.001	0.001	-0.003	0.001	1.793	1.000	0.181

Table A.4 Hypothesis 2: SBSC Promotes Changes in Neural Network Activity
Simple Contrasts

Table 4

Hypothesis 2: SBSC promotes changes in neural activity

Simple Contrasts	<i>Mean Difference</i>	<i>SE</i>	<i>LLCI</i>	<i>ULCI</i>	<i>df</i>	<i>p</i>
DMT partner vs. DMT actor performance at the beginning of the task for negative feedback	-0.138	0.088	-0.310	0.035	1.000	0.117
DMT partner vs. PST dyad member performance at the beginning of the task for negative feedback	0.181	0.072	0.039	0.322	1.000	0.012
DMT actor vs. PST dyad member performance at the beginning of the task for negative feedback	0.319	0.075	0.172	0.465	1.000	0.000
DMT partner vs. DMT actor performance at the end of the task for negative feedback	0.263	0.076	0.113	0.413	1.000	0.001
DMT partner vs. PST dyad member performance at the end of the task for negative feedback	0.293	0.064	0.169	0.418	1.000	0.000
DMT actor vs. PST dyad member performance at the end of the task for negative feedback	0.030	0.064	-0.095	0.155	1.000	0.634

Table A.5 Hypothesis 3: SBSC Affects DMT Actors and Partners Interaction Breakdown

Table 5

Hypothesis 3: SBSC affects DMT actors and partners

Interaction Breakdown	<i>b</i>	<i>SE</i>	<i>LLCI</i>	<i>ULCI</i>	<i>Wald</i>	<i>df</i>	<i>p</i>
Simple 2-way emotion saliency network connectivity x time interaction for the effect of DMT partners on DMT actors	-0.001	0.001	-0.003	0.001	0.884	1.000	0.347
Simple 2-way emotion saliency network connectivity x time interaction for the effect of DMT actors on DMT partners	0.002	0.001	0.000	0.004	3.881	1.000	0.049
Simple 2-way emotion saliency network connectivity x time interaction for the effect of the PST dyad actor on the PST dyad partner	-0.001	0.001	-0.003	0.000	2.412	1.000	0.120
The simple slope of emotion saliency network connectivity for the effect of DMT partners on DMT actors at the beginning of the task	0.059	0.051	-0.041	0.160	1.338	1.000	0.247
The simple slope of emotion saliency network connectivity for the effect of DMT actors on DMT partners at the beginning of the task	-0.087	0.047	-0.179	0.005	3.469	1.000	0.063
The simple slope of emotion saliency network connectivity for the effect of PST dyad members on PST dyad members at the beginning of the task	0.051	0.037	-0.021	0.122	1.945	1.000	0.163
The simple slope of emotion saliency network connectivity for the effect of DMT partners on DMT actors at the end of the task	-0.018	0.050	-0.116	0.079	0.137	1.000	0.711
The simple slope of emotion saliency network connectivity for the effect of DMT actors on DMT partners at the end of the task	0.072	0.053	-0.033	0.176	1.795	1.000	0.180
The simple slope of emotion saliency network connectivity for the effect of PST dyad members on PST dyad members at the end of the task	-0.044	0.039	-0.120	0.031	1.329	1.000	0.249

Table A.6 Hypothesis 3: SBSC Affects DMT Actors and Partners Simple Contrasts

Table 6

Hypothesis 3: SBSC affects DMT actors and partners

Simple Contrasts	Mean Difference	SE	LLCI	ULCI	df	p
DMT partner vs. DMT actor emotion saliency network connectivity at the beginning of the task	1.422	0.706	0.038	2.807	1.000	0.044
DMT partner vs. PST dyad member emotion saliency network connectivity at the beginning of the task	1.528	0.657	0.240	2.816	1.000	0.020
DMT actor vs. PST dyad member emotion saliency network connectivity at the beginning of the task	0.106	0.624	-1.117	1.328	1.000	0.865
DMT partner vs. DMT actor emotion saliency network connectivity at the end of the task	-0.547	0.719	-1.956	0.862	1.000	0.447
DMT partner vs. PST dyad member emotion saliency network connectivity at the end of the task	-1.137	0.658	-2.427	0.153	1.000	0.084
DMT actor vs. PST dyad member emotion saliency network connectivity at the end of the task	-0.590	0.624	-1.813	0.634	1.000	0.345

Table A.7 Hypothesis 4: SBSC Predicts Underperformance Interaction Breakdown

Table 7

Hypothesis 4: SBSC predicts underperformance

Interaction Breakdown	b	SE	LLCI	ULCI	Wald	df	p
Simple 2-way emotion saliency network connectivity to negative feedback x time interaction for the effect of DMT partners	0.001	0.001	0.000	0.002	4.799	1.000	0.028
Simple 2-way emotion saliency network connectivity to negative feedback x time interaction for the effect of DMT actors	0.000	0.001	-0.002	0.001	0.304	1.000	0.582
Simple 2-way emotion saliency network connectivity to negative feedback x time interaction for the effect of PST dyad members	-0.001	0.000	-0.001	0.000	2.880	1.000	0.090
The simple slope of emotion saliency network connectivity to negative feedback for the effect of DMT partners at the beginning of the task	-0.071	0.028	-0.125	-0.017	6.556	1.000	0.010
The simple slope of emotion saliency network connectivity to negative feedback for the effect of DMT actors at the beginning of the task	-0.001	0.027	-0.055	0.052	0.003	1.000	0.959
The simple slope of emotion saliency network connectivity to negative feedback for the effect of PST dyad members at the beginning of the task	0.035	0.017	0.001	0.069	3.966	1.000	0.046
The simple slope of emotion saliency network connectivity to negative feedback for the effect of DMT partners at the end of the task	0.032	0.028	-0.023	0.087	1.298	1.000	0.255
The simple slope of emotion saliency network connectivity to negative feedback for the effect of DMT actors at the end of the task	-0.028	0.030	-0.087	0.030	0.894	1.000	0.344
The simple slope of emotion saliency network connectivity to negative feedback for the effect of PST dyad members at the end of the task	-0.019	0.021	-0.059	0.022	0.829	1.000	0.363

Appendix B

INSTITUTIONAL REVIEW BOARD DOCUMENTATION



Institutional Review Board
210H Hulihan Hall
Newark, DE 19716
Phone: 302-831-2137
Fax: 302-831-2828

DATE: April 29, 2019
TO: Chad Forbes, Ph.D.
FROM: University of Delaware IRB
STUDY TITLE: [473869-21] Learning to Let Go: Why Women are More Likely to Leave STEM Domains
SUBMISSION TYPE: Continuing Review/Progress Report
ACTION: APPROVED for DATA ANALYSIS ONLY
APPROVAL DATE: April 29, 2019
EXPIRATION DATE: May 29, 2020
REVIEW TYPE: Expedited Review
REVIEW CATEGORY: Expedited review category # (3, 4, 7)

Thank you for your Continuing Review/Progress Report submission to the University of Delaware Institutional Review Board (UD IRB). The UD IRB has reviewed and APPROVED the proposed research and submitted documents via Expedited Review in compliance with the pertinent federal regulations.

As the Principal Investigator for this study, you are responsible for and agree that:

- All research must be conducted in accordance with the protocol and all other study forms as approved in this submission. Any revisions to the approved study procedures or documents must be reviewed and approved by the IRB prior to their implementation. Please use the UD amendment form to request the review of any changes to approved study procedures or documents.
- Informed consent is a process that must allow prospective participants sufficient opportunity to discuss and consider whether to participate. IRB-approved and stamped consent documents must be used when enrolling participants and a written copy shall be given to the person signing the informed consent form.
- Unanticipated problems, serious adverse events involving risk to participants, and all non-compliance issues must be reported to this office in a timely fashion according with the UD requirements for reportable events. All sponsor reporting requirements must also be followed.

Oversight of this study by the UD IRB REQUIRES the submission of a CONTINUING REVIEW seeking the renewal of this IRB approval, which will expire on May 29, 2020. A continuing review/progress report form and up-to-date copies of the protocol form and all other approved study materials must be submitted to the UD IRB at least 45 days prior to the expiration date to allow for the required IRB review of that report.

If you have any questions, please contact the UD IRB Office at (302) 831-2137 or via email at hsrb-research@udel.edu. Please include the study title and reference number in all correspondence with this office.